Renewable and Sustainable Energy Reviews 189 (2024) 113792

Contents lists available at ScienceDirect

Renewable and Sustainable Energy Reviews

journal homepage: www.elsevier.com/locate/rser

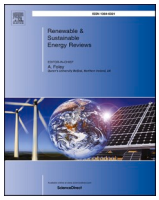

Increasing the resolution of solar and wind time series for energy system modeling: A review

Olalekan Omoyele [a,b,*], Maximilian Hoffmann [a], Matti Koivisto [c], Miguel Larrañeta [d], Jann Michael Weinand [a], Jochen Linßen [a], Detlef Stolten [a,b]

[a] Forschungszentrum Jülich GmbH, Institute of Energy and Climate Research – Techno-economic Systems Analysis (IEK-3), 52425, Jülich, Germany
[b] RWTH Aachen University, Chair for Fuel Cells, Faculty of Mechanical Engineering, 52062, Aachen, Germany
[c] Department of Wind and Energy Systems, Technical University of Denmark, Frederiksborgvej 399, 4000, Roskilde, Denmark
[d] Departamento de Ingeniería Energética Universidad de Sevilla, 4 San Fernando Str, Seville, Spain

ARTICLE INFO

Keywords:
Energy system optimization
Wind speed distribution
Solar photovoltaics
Temporal resolution
Machine learning

ABSTRACT

Bottom-up energy system models are often based on hourly time steps due to limited computational tractability or data availability. However, in order to properly assess the rentability and reliability of energy systems by accounting for the intermittent nature of renewable energy sources, a higher level of detail is necessary. This study reviews different methods for increasing the temporal resolutions of time series data for global horizontal and direct normal irradiance for solar energy, and wind speed for wind energy. The review shows that stochastic methods utilizing random sampling and non-dimensional approaches are the most frequently employed for solar irradiance data downscaling. The non-dimensional approach is particularly simple, with global applicability and a robust methodology with good validation scores. The temporal increment of wind speed, however, is challenging due to its spatiotemporal complexity and variance, especially for accurate wind distribution profiles. Recently, researchers have mostly considered methods that draw on the combination of meteorological reanalysis and stochastic fluctuations, which are more accurate than the simple and conventional interpolation methods. This review provides a road map of how to approach solar and wind speed temporal downscaling methods and quantify their effectiveness. Furthermore, potential future research areas in solar and wind data downscaling are also highlighted.

1. Introduction

Mitigating climate change is part of the Paris Agreement to limit the global temperature increment to $1.5-2^oC$ with respect to the pre-industrial levels [1]. Many countries, therefore, aim to reduce their carbon footprint, with some prominent examples shown in Fig. 1. The power sector, which accounted for 39.3% of total CO_2 emissions in 2022 [2], can only achieve this feat by increasing the share of renewable sources in the energy mix. As an increasing share of intermittent renewable energy and an intensifying interconnection amongst energy sectors has led to a significantly more complex interplay of different technologies, energy system modeling is increasingly employed to support a proper understanding of system rentability and reliability.

Energy system models (ESMs) are used to plan, design, and operate energy systems and explore possible future developments, as well as to assess energy policy options. These models are used to simulate and analyze energy systems' security, rentability, environmental impacts, and different policy options [9]. The history of ESMs dates back to the 1950s, when the first models were designed to help energy planners and policymakers understand the interactions between the different components of energy systems, such as energy production, conversion, and use, with simple assumption-based scenarios [10]. Over the following decades, ESMs evolved as a result of the need for energy security, progress in the computational structures that handle complex problems, and the integration of intermittent renewable energy sources (IRES) [11]. Many ESMs, such as Balmorel, MARKAL, TIMES, EFOM, LEAP, PRIMES, Pypsa, REMix, OSEMOSYS [11,12], and ETHOS.FINE [13] have been designed to optimize energy systems and evaluate the economic, environmental, and social consequences of different energy policies and scenarios. However, ESMs require further development to incorporate more complex structures and methods, with most models

* Corresponding author. Forschungszentrum Jülich GmbH, Institute of Energy and Climate Research – Techno-economic Systems Analysis (IEK-3), 52425 Jülich, Germany.
E-mail address: o.omoyele@fz-juelich.de (O. Omoyele).

https://doi.org/10.1016/j.rser.2023.113792
Received 4 June 2023; Received in revised form 18 September 2023; Accepted 30 September 2023
Available online 6 November 2023

List of abbreviations

ESMs	Energy system models
IRES	Intermittent renewable energy sources
PV	Photovoltaics
GHI	Global horizontal irradiance
DNI	Direct normal irradiance
KNN	K-nearest neighbour
ND	Non-dimensional
ML	Machine learning
ANN	Artificial neural network
GAN	Generative adversarial network
PSD	Power spectral density
MSE	Mean squared error
NMSE	Normalized mean square error
RMSE	Root mean square error
NRMSE	Normalized root mean square error
MBD	Mean biased deviation
KSI	Kolmogorov–Smirnov integral
KLD	Kullback–Leibler Divergence
OVC	Overlapping coefficient

using hourly temporal resolutions.

1.1. Data-driven motivation for sub-hourly time series

Several ESMs, as well as many of the frameworks mentioned above, use hourly time steps to account for the dynamic operation of systems with high shares of IRES [12]. However, higher temporal resolutions have been widely neglected due to two major factors, namely: *data unavailability* and *computational limitations*. Although weather data is globally available at hourly resolutions via reanalysis databases such as MERRA2 or ERA5 [14], other databases focus on small scopes at high resolutions (e.g., the measured ENTSO-e [15] at 15 min intervals for some European countries or weather station data at specific locations). Table 3 in the Appendix displays different open-access wind and solar generation time series databases and their temporal resolutions. Furthermore, sub-hourly modeling of the energy system increases the size and computational complexity of a model. However, coarser data, such as hourly time steps, tends to either underestimate or overestimate ESMs, resulting in unreliable system designs and operating schedules [16,17].

This is because the utilization of hourly-resolved profiles does not necessarily represent the actual stochasticity of real renewable time series appropriately (Fig. 2). For example, Fig. 2 (a) shows that the solar irradiance has a distinct diurnal characteristic, displaying a repetitive curve pattern for both days studied and large intra-hour variability on them. In contrast, the wind speed depicted in Fig. 2 (b) features a less periodic pattern (which will be discussed in section 3.2).

1.2. Relevance of sub-hourly data for energy system models

Studies hitherto have repeatedly attempted to quantify the impact of different temporal resolutions of input time series on ESM results. For this, they have compared the impact of hourly and various sub-hourly resolutions on the dispatch and design of cost-optimal energy systems under the same boundary conditions and assumptions. Gangammanavar et al. [19] incorporated sub-hourly economic dispatch in a stochastic optimization model, in which two different methods for the generation scheduling of the practice were studied at hourly and sub-hourly resolutions of ten, 20, and 30 min. They found that coarse resolutions underestimate the operating costs, comprising the generation costs. In light of substantial penetrations of wind energy, Troy et al. [20] examined whether hourly resolution modeling is adequate or if intra-hourly variability justifies sub-hourly modeling, with 15 min time resolution of unit commitment and economic dispatch. The authors discovered that sub-hourly modeling reveals significantly higher levels of generator cycling, as well as utilization of flexible generation and storage units. Another study found that hourly analyses of energy models underestimate the levels of conventional plant cycling [21]. Energy storage could reduce cycling and improve the efficiency of the system with significant operational cost savings. In an hourly-resolved model, however, the amount of storage plant cycling necessary to reduce system costs is largely underestimated [21].

Pfenninger [16] used downsampling-, clustering-, and heuristics-based approaches to reduce the temporal resolution for a model with high shares of solar photovoltaics (PV) and wind generation

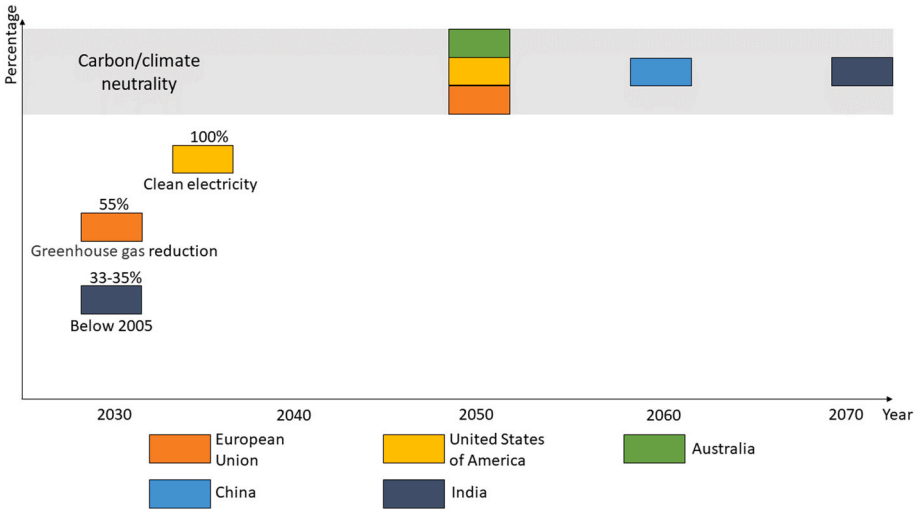

Fig. 1. Carbon emission reduction targets of the European Union, United States of America, Australia, China, and India. The European Union established a target that calls for a greenhouse gas emission reduction of 55% in the economy by 2030 and complete climate neutrality by 2050 [3], with Germany aiming for greenhouse gas neutrality by 2045 [4]. The USA set 2035 as a target for 100% clean electricity, with carbon neutrality no later than 2050 [5]. China, which is the largest CO_2-emitting country in the world, intends to reach peak CO_2 emissions by 2030 and a carbon-free economy before 2060 [6]. The Australian government has also set the target of reducing the country's emissions, with the goal to attain 26–28% below 2005 levels by 2030, and to achieve net zero emissions by 2050 [7]. India also has the goal of reducing its economy's carbon emissions by 33–35% below the 2005 level in 2030 and having net zero carbon emissions by 2070 [8].

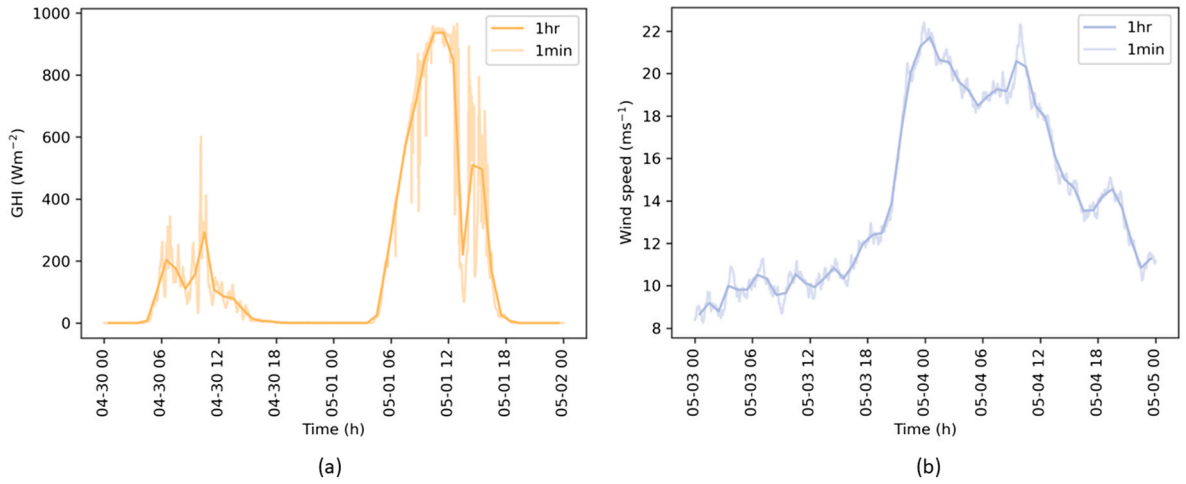

Fig. 2. **(a)** Plot of Global Horizontal Irradiance (GHI) against time at 1 h and a 1 min resolution at a location in Milan, Italy (lat.: 45.5028249, long.: 9.1561092), for two consecutive days. The profile is based on the data from the solar tech lab. [18]; **(b)** plot of the wind speed against time at 1 h and 1 min resolutions at a location in the North Sea (lat.: 51.67, long.: 2.8) for two consecutive days. The profile is based on synthetic data from the CorRES simulation tool (explained in section 3.2).

and concluded that a coarser temporal resolution is unreliable, as the resulting total cost and installed capacities of the energy systems are underestimated. Furthermore, Lopez et al. [22] found an underestimation in the ramping required to maintain the supply/demand balance at an hourly resolution compared to a sub-hourly one. Not only is this the case for energy system optimizations used to determine cost-efficient designs but even more so for the optimization of control systems, where a high temporal resolution is indispensable. For example, the control system of a concentrated solar power plant was analyzed by Meybodi et al. [23], as well as the underestimation of the inverter clipping when high irradiance values are not considered and the performance ratio is overestimated [24–26]. The clipping loss is the lost energy accruing in a PV system due to the inverter moderating its output to meet either its maximum power rating or the maximum allowance power at the grid connection. Clipping is a situation in which the alternating current power output of an inverter is limited due to its peak rating.

Salom et al. [27] investigated the effect of using high-resolution data at one, five, and 12 min intervals versus an hourly resolution in the grid integration analysis of a building with an onsite generation system. The result showed that the difference in peak values computed with hourly and sub-hourly data can be quite significant. Deane et al. [28] present a one-year modeling of the Irish power system with five, 15, 30, and 60 min resolutions using unit commitment and economic dispatch models. Although a more realistic estimation of the total generation cost (approximately 1% higher with 5 min compared to 60) was obtained with resolutions between five and 30 min, the difference was insignificant and the authors concluded that a 30 or 60 min resolution would be sufficient if the system costs alone were of interest. However, when the system's flexibility in terms of ramping and the evaluation of flexible resources such as pumped storage is important, a higher resolution optimization should be selected. Furthermore, Deane et al. [28] and Bistline [29] found out that sub-hourly generation data are necessary for studies with high wind power penetration in the power system in order to accurately capture the ramping effects, start-ups, and load fluctuations.

Kërçi et al. [30] discuss the impact of a sub-hourly unit commitment problem on power system dynamics considering different sub-hourly security-constrained unit commitment resolutions (i.e., five and 15 min) and different wind penetration levels (i.e., 25 and 50%). The results indicate that the higher the wind power volatility, the higher the expected cost due to greater ramping of generating units. Kazemi et al. [31] investigated the effects of different temporal resolutions, such as of five, ten, 15, 30, and 60 min, on generation costs, reserves, and intermittent generators and concluded that for a system with a large degree of renewable penetration, a high temporal resolution is needed for its unit commitment and economic dispatch. This leads to a greater level of system reliability, having captured the intra-hour occurrences of renewable generation. The coarse time steps overestimated the annual generation of a PV plant, thereby reducing the levelized cost of electricity, which is the ratio of the net cost of the system to its expected lifetime energy output by up to 3% [25,32].

Due to computational limits, minutely-resolved datasets are often inappropriate for computationally-demanding applications like multi-objective energy system optimizations [25]. However, complexity reduction techniques like temporal aggregation methods can be used in this case to ensure the computational feasibility of ESMs [11,33,34].

The impact on ESMs combined with the generally poor data availability of sub-hourly profiles of renewables motivates our review. We systematically reviewed the synthesizing of sub-hourly resolutions from hourly ones for the most relevant IRES, i.e., wind and solar energy. As shown in the studies above, most of the modeling and optimization focused on systems with large(r) penetrations of solar and wind energy. The remainder of this review focuses on reducing the temporal resolution of global horizontal irradiance (GHI), direct normal irradiance (DNI), and wind speed, as well as validations and recommendations.

2. Methodology of the literature search

This review summarizes some methodologies used for the temporal downscaling of IRES with a focus on solar and wind time series. GHI, DNI, and wind speed are all paramount for energy system modeling, as they are converted into capacity factor time series data that act as the input parameters of ESMs.

In order to identify relevant articles as shown in Fig. 3, we conducted a systematic hybrid literature research that utilized a keyword-driven search and subsequent citation-driven one. The keyword-based search was carried out in the literature databases Scopus and Web of Science using the following research string:

TITLE-ABS-KEY(("downscale" OR "downscaling" OR "increase temporal resolution") AND ("irradiance" OR "irradiation" OR "wind speed") AND ("data" OR "time series"))

We included articles, conference papers, doctoral theses, and technical reports that deal with methods of downscaling solar irradiance and wind speed. Several were excluded based on title and abstract, as only a few of the identified articles covered the spatial downscaling of solar irradiance or wind speed. Others, which only quantified the impact of the sub-hourly data on energy system modeling, as shown in section 1.2,

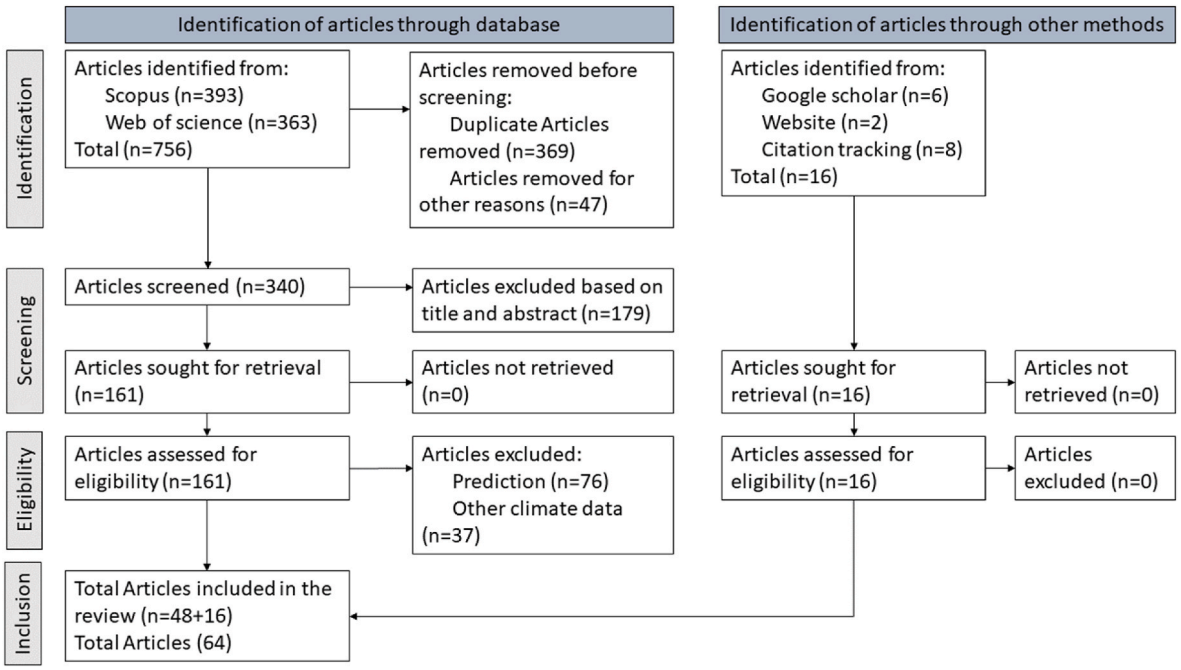

Fig. 3. Flow diagram of the systematic literature review based on the PRISMA scheme.

were not considered relevant. We also excluded articles that downscale other meteorological data, dynamic downscaling, and articles that are based on predictions instead of downscaling. Overall, 48 articles from our literature search met the requirements for inclusion, as shown in the *Preferred Reporting Items for Systematic Reviews and Meta-Analyses* (PRISMA) [35] workflow in Fig. 3. An additional 16 publications were identified in manual searches through other methods such as web searches, e.g., with Google Scholar and citation tracking. The summary of the articles related to solar energy has been presented in Table 2.

3. Methods for increasing time series resolution

The methods discussed in this review focus on the input time series data of solar and wind for energy system optimization. An overview of the downscaling methods used is shown in Fig. 4, in which the methodology is segmented into solar (GHI, DNI) and wind energy (wind speed). In order to be able to downscale the time series of meteorological data, the condition of the atmosphere must be understood. The clearness index or clear sky index is an important parameter used for downscaling approaches to normalize solar irradiance based on sky parameters. The clear sky condition is used to determine the irradiance reaching the earth's surface without taking cloud cover into account. This clearness index is classified into different classes in order to categorize irradiance based on the condition of the sky. Subsequently, Markov, deterministic, stochastic, non-dimensional, or machine learning approaches were used for downscaling to increase the temporal resolution (see section 3.1). The wind speed was downscaled using stochastic approaches or power spectral density (PSD) (see section 3.2). The resolved data was then compared with real measured data from weather stations for validation. Several approaches for error measurements between the synthetic and measured data are discussed in section 4.

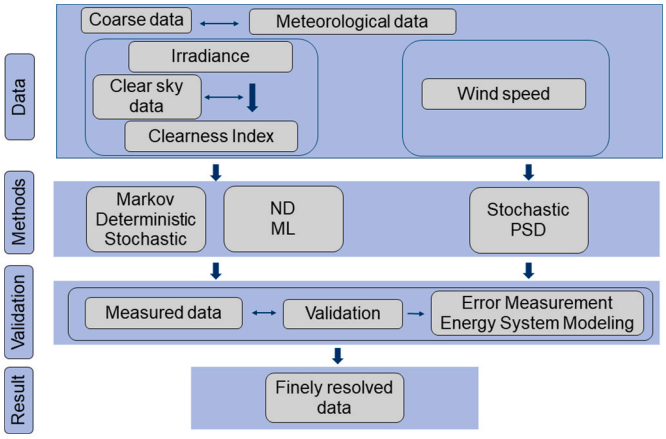

Fig. 4. Overview of methods for downscaling time series data identified in the review and the connections to obtain highly resolved data. The methods for downscaling solar irradiance include Markov, deterministic, stochastic, non-dimensional (ND), and machine learning (ML) approaches. The methods for wind speed include stochastic approaches and power spectral density (PSD).

3.1. Solar energy

With respect to solar energy, several methods have been analyzed and reviewed in Refs. [36–38], which estimate the clear sky model of different resolutions based on various parameters including relative humidity, zenith angle, aerosol concentration, temperature, air pressure, and Rayleigh scattering. The clearness index, k_t, is used to model the variability of the sky irradiance based on the cloudiness of the sky at a certain time t. It is an important index on which many temporal downscaling approaches depend. The clearness index is the ratio of the energy incident on a collector with the atmospheric effect to the energy incident on a collector without the atmospheric effect. The index k_t is then the ratio of the measured irradiance H to the clear sky irradiance H_e, and is location-dependent Eq. (1):

$$k_t = \frac{H}{H_e} \tag{1}$$

The clear sky index is the bedrock on which many approaches are built. The following subsections analyze the methods for downscaling solar irradiance.

3.1.1. Markov chain approach

The Markov approach is based on the Markov property, that the

probability distribution of the future state of a process is conditionally-independent of the past of the process other than the present (a detailed explanation of the Markov model is described in Appendix C). In the downscaling process that uses the Markov approach, the clearness index of the higher temporal scale to be downscaled to is calculated. It is then classified into different states based on the irradiance values representing the cloudiness of the atmosphere. The probability of different hours in each of the states is calculated, leading to the construction of the Markov transition matrix. The k_t of the irradiance to be downscaled is computed and fitted based on the weighted probability of the Markov transition matrix. The downscaled k_t is then converted into the irradiance using Eq. (1), above.

In the following, Markov chain approaches for the temporal downscaling of solar irradiance are presented. The methodological concept of Markov chains can be found in Appendix C. Ngoko et al. [39] grouped days based on their cloudiness by determining the daily clearness index, k_d, and created a Markov transition matrix for each of the groups of k_d. The order of the Markov time series synthesis model to be used can also be seen by the partial autocorrelation function of the time series. The order of the Markov chain refers to the number of previous states considered when predicting the future one. Ngoko et al. [39] employed a simple Markov time series synthesis model to downscale the GHI by removing its dependence on the zenith angle and transforming it into a normalized clearness index. A Markov transition matrix was created for three different conditions (cloudless, broken clouds, and overcast) [40]. A clearness index of 0.01 intervals and discrete-time Markov chains was then applied to downscale the GHI from 1 h to 1 min. The seasonality, as well as the diurnal and pressure influences on the cloud cover, were taken into account by Bright et al. [41] and on the basis of this, further used to synthesize a 1 min global irradiance from hourly weather data such as pressure, wind speed, and cloud amount to estimate the amount of cloud cover and the cloud height [42,43]. The authors later extended the method to the spatial dimension, resulting in a spatially-decorrelated solar irradiance generator [44]. Bright [45] evaluated several GHI training datasets to generate a more accurate systematic Markov transition matrix and an arbitrary number of states for the Markov transition matrix on clear-sky index data [46]. Martins et al. [47] downscaled GHI from 1 h to 1 min using the Markov approach clearness index based on cloudy, partly cloudy, and clear sky conditions. Munkhammar and Widén [48,49] used their approach in Ref. [46] to model the 1 min beam, diffuse, and global clear sky solar irradiance from hourly global irradiance. In turn, Shi et al. [50] considered that the irradiance of a highly polluted area can be reduced as a result of airborne pollutants that form a layer of cloud in the form of particles that block, absorb, and scatter irradiance. They extended the clear sky model used by Bright et al. [41] to accommodate irradiance in highly polluted regions using aerosol optical depth and the quality of the air index.

Frimane et al. [51] proposed a method for downscaling a feature- and satellite-based database measured in a 10–20 min irradiance time series to 1 min. For the clearness index, they used an automatic classifier clustering method based on a non-parametric Bayesian approach. This captured more variability with a lower error compared to others [41,42]. Inacio et al. [52] adopted the dependence of the clearness index on the predominance of clouds over a certain time interval using an automatic cloud classification procedure with satellite images to downscale GHI and DNI from 1 h to 1 min.

3.1.2. Deterministic approach

Deterministic approaches comprise linear and cubic methods for interpolating data. Linear interpolations work as follows: suppose that two points on a graph, (x_0, y_0) and (x_1, y_1) are given and values need to be estimated between these two. If the points are not equally spaced, there is a gap between them. In this case, we wish to estimate a value, say, y, of a point x. The value of y is obtained by finding a linear combination of x_0 and x_1 that results in x, as seen in Refs. [45,53–56]. The interpolation methods are used for the deterministic approach before introducing fluctuations or randomness to better capture the variability of the intra-hourly time series. Linear interpolation is the simplest method used, whereas cubic interpolation can provide smoother edges and more accurate interpolation results. The linear interpolation method is used by Buster et al. [57] to downscale the National Solar Radiation Database (a collection of serially-complete meteorological and solar irradiance datasets) [58] from 30 min to 5 min and 1 min. The spatial resolution of the coarse data was first increased, following the method of the National Solar Radiation Database [58]. Then, a temporal linear interpolation was employed. Furthermore, McDowell and Kummert [54] and McDowell et al. [55] applied an improved linear interpolation algorithm to different building performance programs (EnergyPlus, TRNSYS17, and TRNSYS18) for creating sub-hourly resolved time series. The algorithm was developed with a reliance on the result of the previous period to calculate the next phase. A linear interpolation approach was later developed by Zhang et al. [56,59], who classified irradiance into clear and non-clear days and linearly interpolated the former. A detailed explanation of this method is presented in section 3.1.3. Pereira et al. [60] also employed a bi-linear interpolation to downscale an hourly European center for medium-range weather forecast data to 30 min.

Cubic interpolation uses a cubic polynomial instead of a linear polynomial. The cubic interpolation has the general form of $y = a_0 + a_1x + a_2x^2 + a_3x^3$, where a_0, a_1, a_2, and a_3 are known coefficients. In cubic interpolation, the equation is solved for these coefficients and then y is estimated to obtain a smooth curve with which intermediate values can be imputed. The cubic interpolation technique was applied in several studies [61–63] to derive patterns or profiles that are superposed by stochastic fluctuations. Ruiz-Arias [64] considered a cubic interpolation that preserves the mean of the datasets. They used the second order cubic polynomial to reduce the variations in the synthetic data. Another method of piecewise cubic interpolation was used by Balog et al. [65] to downscale irradiance from 1 h to 1 min. The authors reported that the cubic interpolation was only suitable for clear days and that non-clear ones were not suitably captured. The method was then further developed to use sinusoidal interpolation, as proposed by the authors to achieve a higher degree of accuracy than ordinary cubic interpolation.

3.1.3. Stochastic approach

Some articles add stochasticity to the deterministic results presented above, such as that of Polo et al. [63], which added randomness to the cubic interpolation. They fitted the sky conditions in the form of the clearness index to a beta distribution to downscale both the GHI and DNI from 1 h to 10 min. Moreover, randomness was added to the deterministic result from the cubic interpolation by fitting the sky conditions in the form of the clearness index to a beta distribution in order to downscale both the GHI and DNI from 1 h to 10 min. The method was further developed in Refs. [61,62], using and normalizing an improved model by Skartveit and Olseth [66] for the clearness index. The method also covers hazy days by using perturbations.

Grantham et al. [67] extended the work by Polo et al. [63] by using and categorizing a clear sky ratio between sunrise and sunset instead of the normalized clearness index. A bootstrap method to generate five-minutely synthetic DNI data from hourly datasets was used instead of fitting clearness to a beta distribution, as was undertaken by Polo et al. [63]. In a later publication, Grantham et al. [68] employed the same bootstrapping technique to also downscale hourly GHI data to 5 min. Wey et al. [69], in turn, created a set of daily profiles using the measured ground-based data of a location of interest. They then generated a solar irradiance time series at a resolution of 10 min via fusion by searching for the closest day possible through the Euclidean distance between each hourly data point to be downscaled and the stored profiles. Frimane et al. [70] utilized the Dirichlet distribution to model the distribution of minute-level irradiance through the clearness

index, displaying a similar variability as the high-resolution data. They covered the Köppen–Geiger weather classification, making it globally applicable. Keeratimahat et al. [71] accounted for the spatial smoothening effect by combining data following the clear sky index and scaled the distribution of the measured variability in accordance with the ratio of reference and simulated photovoltaic plant capacities. A scaled distribution of the equivalent clear sky condition was then adopted to create a time series of 4 s PV outputs by random sampling. The spatial variability of the hourly time series, which was gridded around the location of interest, was used by Perry and Troccoli [72] to downscale the solar GHI data to 1 min. Each hour was classified into six groups based on the standard deviation and distance-weighted average. Two methods were then applied to downscale to 1 min time series data, low and mean variability classes, or a high variability one. The classes with high variability were modeled as transitions between the varying degrees of the opacity of the cloud and the states of clear skies. The mean or low classes (classes 1–4) were modeled using an autoregressive time series synthesis model. The autoregressive time series synthesis model was also adopted with a clearness index in Beyer et al. [73] to downscale DNI time series data from 1 h to 1 min. The autoregressive time series synthesis model is a mathematical one that has been used in many forecasting scenarios, including meteorology, to forecast weather. In this approach, a future value is predicted based on past values. The previous value is termed 'lag'. In order to determine the lags that will have a high impact on the future value, the autocorrelation and partial autocorrelation of the time series were determined. The autoregressive time series synthesis model was then used to predict the intra-hour clearness index of solar irradiance.

Zhang et al. [59] classified the GHI into clear days and non-clear ones with the assumption that there is a similarity in the variability of the clear day GHI and the actual GHI, instead of using a complex algorithm to determine the clear hours of the day. The distinction was adopted by linearly interpolating the National Solar Radiation Database data and identifying the first difference between the interpolated hourly data and the clear sky data. The maximum, y, of the difference between the two, was tested over a tolerance. If $y < 0.1$, it meant a clear day and if $y > 0.1$, it meant a non-clear one. The clear day was linearly interpolated, which yielded a better result than the stochastic approach in this regard. The non-clear day was modeled with errors between the measured and the interpolated data, which were both log-additive non-gaussian mixtures. Zhang et al. [56] further developed the method presented in Ref. [59] to capture excursions in irradiance, which is the period at which the irradiance shoots above the theoretical clear sky as a result of scattering events. In three consecutive publications, Zhang et al. [56,59,74] developed methods updated in the third [74], adopting the methods of [56,59] to create an automatic temporal downscaling classifier using a log-additive model. The model comprises an error function that helps to model variability and a Bernoulli random variable that can detect whether or not the sky is clear.

Widén and Munkhammar [75] used the Gaussian copula, which is based on the assumption that variables are jointly normally distributed and can be dependently represented by a correlation matrix to temporally- and spatially-downscale an hourly solar irradiance to 15 s. The Gaussian copula is also applied by Huang et al. [76], whereby the hourly clearness index is downscaled with the retainment of the original spectral density. Matthew and Andrew [77] incorporated the sub-hourly solar variability from Hummon et al. [78] to downscale the National Solar Radiation Database data for up to 1 min. The method is based on spatial patches between measured sites that represent the sky conditions.

3.1.4. Non-dimensionalization of solar irradiance approach

The non-dimensional approach uses the scaling of irradiance data by converting it into a non-dimensional parameter measured against time. In this respect, the daily irradiance of a location is divided by its clear sky condition to create a scale of irradiance between 0 and 1. The scaling process is also performed for the universal time between sunrise and sunset. The ratio of the elapsed universal time to the day length normalizes the time to values between 0 and 1. A database exists that stores the daily plot of the non-dimensional irradiance against the non-dimensional time, as is shown in Fig. 5. A minimum of one year of daily profiles for non-dimensional irradiance over non-dimensional time is required in the database for the location of interest. The hourly/daily data to be downscaled is then compared to the hourly/daily data of the database and the most similar data, i.e., the closest data possible in terms of the distances between the measured data to be downscaled and that in the database, is selected.

To the best of the author's knowledge, the non-dimensional approach of modeling daily irradiance curves was first introduced by Peruchena et al. [79], who modeled the clear sky conditions with a curve fitting. Then, the sub-hourly model was fitted into the daily curve of the location by calculating the closest Euclidean distance to the curve possible.

The non-dimensional approach is based on the stance of the seasonality of the solar irradiance and the assumption that the measured annual data of the location can dynamically produce multiple years of irradiance of the same resolution as the measured data [53,80–82]. The methodology was applied in a desert location [80], as well as in different climatic zones [53], and also directly in Fernández-Peruchena et al. [83] and Poole and Dinter [84] to downscale the DNI.

Larrañeta et al. [61,85] considered the non-dimensionalization of the irradiance by creating daily curves of non-dimensional DNI and non-dimensional time. The authors developed the method by Peruchena et al. [79] to improve its global applicability by adopting the database to accommodate the five major Köppen–Geiger weather classifications. They also employed more parameters to accommodate the variability index (the ratio of the length of the measured irradiance to that of the clear sky irradiance), distribution and energy in the database and classified it using the K-nearest neighbour (KNN) machine learning method to find the closest distance. Drawing on the work of Larrañeta et al. [61,85,86], Larrañeta et al. [87] developed an ND tool [88] that downscales hourly DNI and GHI time series data to 1 min. This tool was applied by Jiménez-Valero et al. [89] as the last step in a method for synthetically generating the plausible meteorological years of 1 min GHI and DNI data from hourly datasets. The authors utilized non-parametric bootstrapping and an autoregressive model to synthesize the daily time series. A large database of multiple years was used, which was based on the DNI characterization by Moreno-Tejera et al. [90] for retrieving the distribution, variability, and energy.

Although the method by Peruchena et al. [53,80–82] is location-specific or location-dependent based on the historical data of the location and is computationally-intensive, the method of Larrañeta et al. [61,85–87,89] does not require historical data.

3.1.5. Machine learning approach

Machine learning algorithms are mostly applied to the prediction of future irradiance, with only a few being applied to downscaling solar irradiance. Some machine learning algorithms have also been used in the classification of the clearness index, as well as in Larrañeta et al. [61], where the KNN algorithm was used to classify 1 min irradiance in the database to similar days. Two methods used in the literature on the basis of artificial neural networks (ANNs) and generative adversarial networks (GANs) are presented in this section.

An ANN is a data model that is inspired by biological neural networks, such as the human brain [91]. A huge number of intricately-linked processing units (neurons) make up ANNs, which collaborate to solve certain problems. These networks are adaptable, which means that they can modify their structure in response to information passing through the network, both internally and externally, while it is in use. Examples of the applications of ANNs include character recognition, face recognition, speech recognition, and automated-driving cars [92].

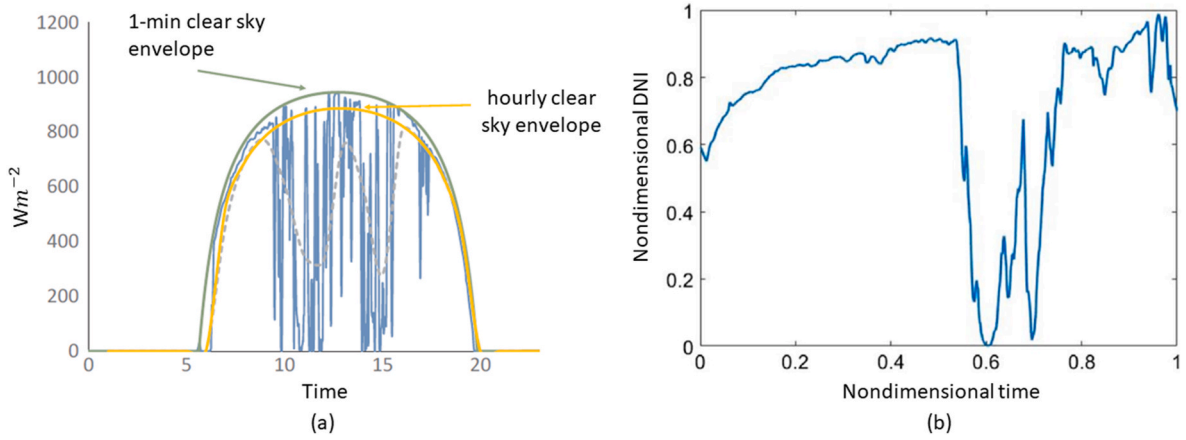

Fig. 5. **(a)** Measured 1 min DNI with its enveloping curve; **(b)** non-dimensional DNI curve reprinted from M. Larrañeta, C. Fernandez-Peruchena, M. A. Silva-Pérez, and I. Lillo-Bravo, "Methodology to synthetically downscale DNI time series from 1-h to 1-min temporal resolution with geographic flexibility," Solar Energy, vol. 162, pp. 573–584, 2018 [61]. Copyright (2018), with permission from Elsevier.

ANNs can be used for the classification process of solar irradiance sky conditions, as shown in Fig. 6. The cloud-related properties defining the clearness index or satellite-based cloud parameters can be classified using neural networks. Based on this, a random sample is generated that is compared to highly-resolved data in a database.

The ANN method was used by Schreck et al. [93] to classify the variability amongst satellite imagery by feeding the measured data and cloud parameters as the inputs of a feedforward multilayer neural network, which was then normalized. Every 15 min, a satellite image was obtained from which the cloud parameters were produced. A database created by Schroedter-Homscheidt et al. [94], which consists of minutely-resolved measured irradiance parameters representing some specific hours in different locations, was used. The hourly time series to be downscaled is matched with the 1 min time series from the database, which produces synthetic irradiance in minute resolution when multiplied by the clear sky irradiance. Rodríguez et al. [95] also applied a deep neural network, which is a neural network with more hidden layers than ANN [96] to estimate the DNI at 1 min in any location. The authors used 1-min data for the same location class, as defined by the Köppen-Geiger.

A new type of network called GAN has been proposed for data synthesis. GANs were first developed in 2014 [97], and consist of two separate networks competing against each other: a generator and a discriminator [98], as shown in Fig. 7. The goal of GANs is to generate new and realistic samples from a target distribution if the original training data is not available [97]. A random noise z is sent to the generator to create synthetic data that tends to fool the discriminator. The discriminator detects the synthetic data and compares it with the high-resolution data from the measured values. GANs can be used to solve any tasks that can be posed as a generative modeling problem, such as image generation, style transfer, audio generation, and natural

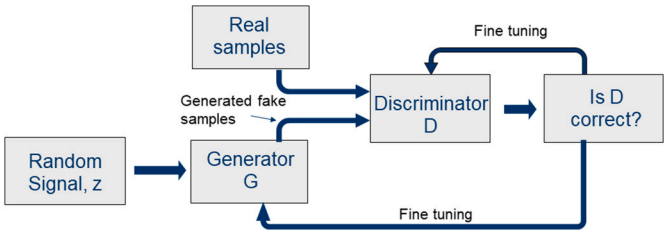

Fig. 7. Structure of generative adversarial network.

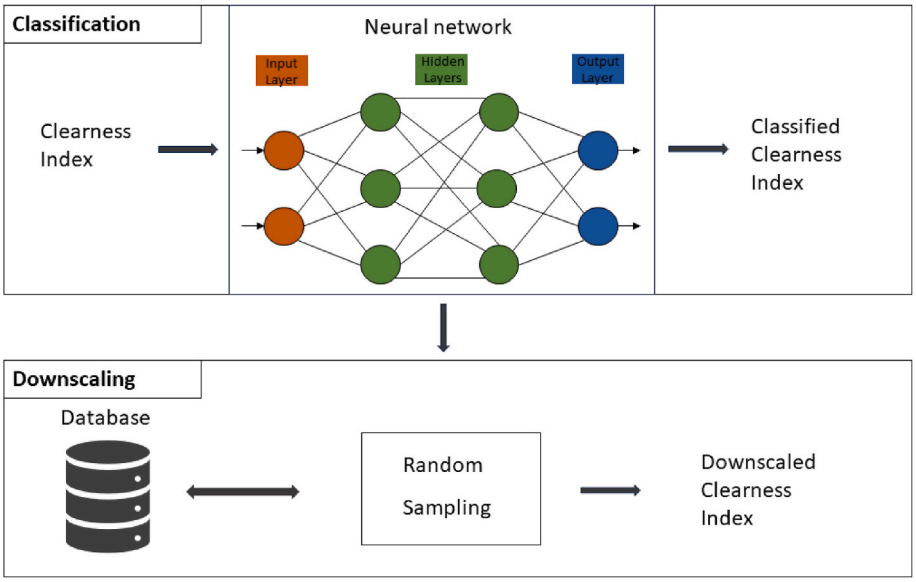

Fig. 6. Machine learning downscaling approach.

language generation [99]. However, to the best of the authors' knowledge, their application to weather time series generation has not yet been thoroughly investigated. In the field of time series generation, GANs have been extensively used in the data imputation of missing meteorological data [100–103]. However, the concept of GAN was applied by Tang et al. [104] to the downscaling of PV power data from 30 min and 1 h to 5 min. To the best of our knowledge, this is the first application of GAN to the downscaling of time series. In the method, measured (fine-resolution irradiance) data was compared to the low-resolution (hourly or 30 min irradiance) data in the generator. In place of the random noise that serves as an input in the generator, a low-resolution irradiance was used that was compared with the measured irradiance in the generator.

Renewable energy forecasting plays a vital role in shaping the future of clean and sustainable energy, energy management, and efficient grid operation [105]. The machine learning method is essential for forecasting different time resolutions. As the future ESM relies more accurately on sub-hourly data [27], several authors have applied the machine learning approach to future prediction or forecast. For instance, Kreuwel et al. [106] forecasted 1 min day ahead solar irradiance from the coarse hourly data using the probability density function of irradiance. Karasu and Altan [107] also predicted solar irradiance using different meteorological parameters (i.e., solar radiation, temperature, humidity, barometric pressure, wind speed, wind direction, and sunrise/sunset) in machine learning using a random forest to deal with nonlinear dynamics in the data. Several other forecasting methods have been detailed by Benti et al. [105] and Assaf et al. [108].

3.2. Wind energy

The wind speed does not follow a specific daily profile as in the case of solar DNI and GHI, which exhibit a strong periodic diurnal pattern (see Fig. 2 (b)). As there is much less literature on wind speed downscaling, in this section we present all existing methods without highlighting individual approaches in the subsections.

Even though few methods deal with the wind speed downscaling process, a plethora of research addresses the spatiotemporal reanalysis of wind speed by using high-quality observations and numerical weather prediction models. To address the limitations of reanalysis data and improve the accuracy of wind speed estimates, researchers have developed dynamic downscaling methods that take into account local subdiurnal meteorological effects [109]. These dynamic downscaling methods utilize high-resolution regional simulations for dynamically extending the impacts of global climate models to regions [110]. However, despite their effectiveness, dynamic downscaling methods have certain limitations. One limitation of dynamic downscaling methods is their increased data requirements [111]. Another is the need for extensive computational resources to handle the substantial amount of data entailed by dynamic downscaling [111]. To overcome these limitations, some researchers have focused on developing statistical temporal downscaling methods for wind speed characteristics [111].

Several studies have considered the probability density function of wind speed, both onshore and offshore, to fit in wind speed distributions. A review of the probability density function was conducted by Carta et al. [112], in which different wind speed probability density functions were fitted into statistical distributions such as gamma, Rayleigh, Weibull, normal, inverse gaussian, and beta distributions with varied distribution parameters. The authors concluded that the two-parameter Weibull distribution is acceptable and the most widely used distribution based on an analysis of the goodness of fit of the cumulative density function of the wind data. However, it was stated that the Weibull distribution does not suitably model a null wind speed because it is defined for positive values only. Furthermore, the Weibull distribution is not well suited to modeling bimodal wind speed distributions, in which the wind speed has two distinct peaks as a result of the complex interactions between meteorological and topographical factors. After the review of Carta et al. [112], Jung and Schindler [113] also reviewed the wind speed distribution for papers between 2010 and 2018, confirming the conclusion of Carta et al. [112]. In their work, they focused on studies with more than one fitted parametric distribution. The non-parametric distribution articles were not considered because of the similarities to the Weibull distribution. In particular, the two-parameter (scale and shape) Weibull distribution is widely used. The wakeby (five-parameter) and kappa (four-parameter) distributions were indicated as better distribution functions based on the goodness of fit, parameter estimation, and distribution. However, it is difficult to obtain a single distribution that can universally represent the wind speed distribution [113].

The concept of wind speed distribution was adopted by Shin et al. [111] to downscale the daily statistics of wind speed to 1 h and 10 min Weibull distributions. Carapellucci and Giordano [114] also used the statistical distribution of the wind speed to downscale monthly average wind speeds to hourly ones. The authors increased the resolution by creating a deterministic pattern generated using an autoregressive model of the first order. Deterministic and stochastic components of the time series were then added to fit into a Weibull distribution. Even though Carapellucci and Giordano [114] used statistics to model wind speed, Olauson et al. [115] claimed that it is inaccurate to measure wind speed using solely a statistical model. Some of the problems inherent to a purely statistical model include the complexity of wind speed, which is influenced by several factors including terrain, vegetation, and atmospheric conditions. Other problems include the non-stationarity and non-linearity of wind speed, its spatial variability, and dependence on a complex physical process. Therefore, it is advisable to not downscale wind speed using a purely statistical model, as it is a complex physical process that requires a combination of statistical, physical, and numerical models. Following this, Olauson et al. [115] concluded that a physical downscaling approach should be used that combines information from meteorological models and observational data, which can provide more accurate results.

Olauson et al. [115] used the hourly data from a meteorological model with fluctuations from stochastic simulations. The authors employed the PSD of the periods to study the fluctuations. A cubic interpolated value from the hourly meteorological observation was subtracted from the ground-based values to capture the fluctuations, which were then adjusted to stationarity. A fast Fourier transformation was used to convert the result into the frequency domain on which appropriate magnitude and phase angle adjustments were made. The adjusted value was subsequently transformed using the inverse fast Fourier transformation. The high-resolution value is the sum of the interpolated value and the fluctuation. Although the method by Olauson et al. [115] modeled the variability, the authors assumed that the stationarity approach used for the location observed would apply to every other location.

The CorRES tool [116], which is a flexible simulation tool that uses correlation-based methods to model renewable energy systems, was employed by Koivisto et al. [117]. They combined meteorological data from reanalyses and stochastic fluctuations, as in Olauson et al. [115], to downscale wind speed from hourly to 15 min resolution in Koivisto et al. [117], or up to 5 min in Murcia Leon et al. [118]. A simple diagrammatic representation of the process is shown in Fig. 8. The major development was to capture the threshold frequency at which the reanalysis data captures the variability. The simulated fluctuations from the stochastic model were then added to the reanalysis data on the high frequencies (considering the threshold frequency above which the variability of the reanalysis data is inadequate).

The effect of turbulence was critically considered by Schillebeeckx and Leroy [119]. They extended the mesoscale spectrum with a spectral correction of the smoothening effect, leading to an underestimation of the hourly variability in the weather research and forecast hourly data. A correction frequency was also determined, as in the case of Koivisto et al. [117], beyond which a correction was applied to the weather data

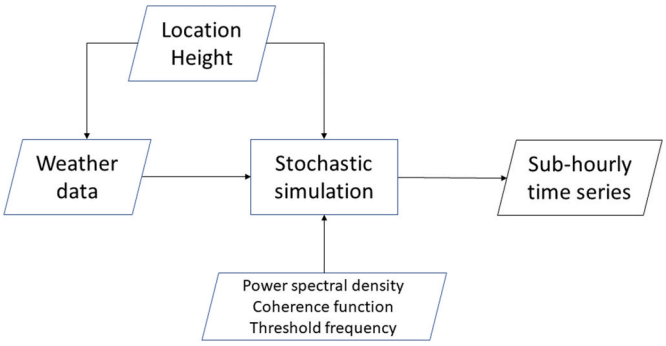

Fig. 8. Generic flow diagram of the wind speed downscaling process as used by Refs. [117–119]. The power spectral density for an individual location will show the distribution of the wind speed to the frequency components, with the coherence function being calculated based on the distance between the locations (more information about the coherence functions can be found in Sørensen et al. [120]).

(e.g., from reanalysis datasets), in the frequency domain. A full-scale spectral model with turbulence at an arbitrary rate was produced in a microscale model. The combination of the corrected mesoscale and the full-spectral microscale models yields a temporally-downscaled wind speed time series. Kumar et al. [121] utilized a neural network with global climate model outputs and meteorological observations to downscale monthly meteorological variables (wind speed, radiations, pressure, humidity, precipitations, and temperature) to six-hourly data. However, the concept of machine learning has mostly been applied to wind speed for predictions [122–124].

4. Data validation

Different methods for downscaling the time series of solar irradiance and wind speed were introduced in subsections 3.1 and 3.2. The accuracy of the downscaled data is typically validated by comparing it with the real data of a location for which measured data is available.

The most frequently used methods to compare synthetic and measured data in the literature are the mean squared error (MSE), normalized mean square error (NMSE), root mean square error (RMSE), normalized root mean square error (NRMSE), and the Kolmogorov–Smirnov integral (KSI) test.

The MSE is a statistical measure of the accuracy of a dataset [125]. It can be thought of as the average amount by which the square of each synthetic data point differs from the measured value. The NMSE is the MSE that is normalized between the maximum and minimum values of the measured data. The MSE and NMSE can be represented mathematically by Eqs. (2) and (3), respectively:

$$MSE = \frac{1}{n}\sum_{i=1}^{n}(y_i - \hat{y}_i)^2 \quad (2)$$

$$NMSE = \frac{\frac{1}{n}\sum_{i=1}^{n}(y_i - \hat{y}_i)^2}{y_{max} - y_{min}} \quad (3)$$

y_i is the observed data, $\hat{y}_i$ the synthetic data, y_{min} and y_{max} are the minimum and maximum values of the observed data, respectively, and n is the number of data points.

The RMSE is a variant of the MSE, providing the root of the squared errors between the measured and synthetic data [126]. The RMSE is mathematically-related to the standard deviation of the dataset. The RMSE is most commonly used in the context of statistical regression, in which it is used to measure the accuracy of a statistical model. The NRMSE is the RMSE, which is normalized between the maximum and the minimum values of the measured data. The RMSE and NRMSE can be mathematically represented by Eqs. (4) and (5), respectively:

$$RMSE = \sqrt{\frac{1}{n}\sum_{i=1}^{n}(y_i - \hat{y}_i)^2} \quad (4)$$

$$NRMSE = \frac{\sqrt{\frac{1}{n}\sum_{i=1}^{n}(y_i - \hat{y}_i)^2}}{y_{max} - y_{min}} \quad (5)$$

The NMSE and NRMSE above are normalized over the range, and can also be normalized over the mean and standard deviation [127].

The KSI is used to test for the difference in the shape of two sample distributions. It tests for the overall shape of the distribution or the cumulative distribution function and is not only related to the measure of tendency, a measure of dispersion, although the measures also affect the overall shape of the distribution. The KSI can be represented by Eq. (6) and encompasses taking the integral of the maximum absolute difference between the two cumulative distribution functions (the measured time series data and the synthetic time series data) over the extreme values of the independent variable:

$$KSI = \int_{x_{min}}^{x_{max}} |F(x) - G(x)|\, dx \quad (6)$$

The F(x) is the observed data, G(x) the synthetic data, and x_{min} and x_{max} are the minimum and maximum values of the observed data, respectively, whereas the KSI can be converted into a percentage, as used by Fernandez-Peruchena et al. [53] and Larrañeta et al. [61], and is represented by Eqs. (7)–(9).

$$KSI = \frac{\int_{x_{min}}^{x_{max}} |F(x) - G(x)| dx}{a_{critical}} \quad (7)$$

$$a_{critical} = V_c(x_{max} - x_{min}) \quad (8)$$

$$V_c = \frac{1.63}{\sqrt{n}}; \quad n \geq 35 \quad (9)$$

V_c is referred to as the critical value, as it is sample size-dependent and n is the number of data points. The V_c is calculated with a 49% level of confidence [61]. The RMSE and mean-biased deviation (MBD) as a measure of dispersion and the KSI as a measure of distribution combined provide a good indicator of the validation [53], which makes them more frequently used.

Some other validation methods include Kullback–Leibler Divergence (KLD), which is a mathematical method used to measure the difference between two probability distributions. The KLD measures the amount of information lost when approximating one probability distribution with another. The KLD has applications in the validation of synthetic irradiance time series [128]. Another method of time series validation is the overlapping coefficient (OVC), which measures the degree of overlap between two or more time series. It can be used to assess the correlation of two variables to compare the similarity of two time series. An OVC of one indicates that the two series are completely correlated, whereas an OVC of 0 indicates no correlation [128]. When comparing two distributions, the OVC accounts for the number of events shared by the two distributions under comparison, whereas the KLD assesses the number of events that are shared by both distributions, and both can be employed. The KLD and OVC are represented by Eqs. (10) and (11), respectively, as highlighted by Frimane and Bright [128]:

$$KLD\,(f\|g) = \int F(x)\, log\left(\frac{F(x)}{G(x)}\right) dx \quad (10)$$

$$OVC\,(f,g) = \int min\,[F(x), G(x)]\,\mathrm{dx} \quad (11)$$

The autocorrelation function can be used to study the accuracy of the synthetic data by examining whether there is a correlation between data

points at different time intervals. These varying time intervals plotted from both the synthetic and measured data can be compared for temporal dependence. Furthermore, the PSD of the measured and synthetic data can be plotted for an accuracy comparison. The MSE or RMSE can then be further applied. Another metric for the PSD is the area covered by the logarithm of the PSDs of the synthetic and measured data [115]. Some other validation tests that can be used include the mean, standard deviation, skewness, kurtosis, R^2, MBD, ramp rate, Nash–Sutcliffe efficiency, the Willmott index of agreement, and Legates coefficient of efficiency. Several researchers have used different validation methods for their analyses and the most common methods used are the RMSE and KSI. The analysis of the validation methods is shown in the table of literature, Table 2. The table also displays the site dependency of each of the studies evaluated, which is taken as viable if the ground data of the location to be downscaled is required for the method.

5. Discussion

Sub-hourly data use in energy system models is gaining importance, as it helps improve forecasting and planning, as well as enabling better grid integration of renewable energy sources [27]. Sub-hourly data can be used to assess the impact of wind and solar energy production on the grid, including the risk of imbalances between energy supply and demand [21]. This information can help in the development of strategies for integrating renewable energy into the grid more effectively and support the deployment of ancillary services, such as demand response or energy storage to maintain grid stability [21]. Different methods have emerged to increase the temporal resolution of IRES, with methods for solar and wind time series being the two most relevant for renewable ESMs. The solar irradiance, DNI, and GHI have strong seasonal and diurnal characteristics, hence the reason why a minimum of one year of data is needed for the downscaling process [61]. Even though both solar and wind have seasonal attributes, wind speed does not have a simple diurnal characteristic and statistical distribution.

Several researchers have worked on methods to increase the temporal resolution of IRES , a research area constantly gaining momentum, with a positive trend in the methods analyzed in Fig. 9(a). The stochastic method analyzed in the trend encompasses the Markov chain approach and the stochastic processes described in section 3.1.3 other than the Markov chain. The deterministic approach was not considered in the trend, because it is mostly used alongside the stochastic approach to create a pattern for the stochastic fluctuations. The deterministic approach (linear and cubic interpolations) is an easy yet ineffective means of downscaling. Although linear interpolation uses a linear relationship to fit several datasets between two irradiance data points, the fitted values can only lie between the two values used for the interpolation. Therefore, the extreme points in the data that have been averaged out are not captured by linear interpolation. The cubic interpolation partially avoids this downside by using a cubic relationship that can yield synthesized extreme values being larger or smaller than those used for the fitting. Depending on the method used, the stochastic approach is computationally-intensive and introduces inherent uncertainties that emanate from the risks of using randomness, which may produce different outcomes across multiple simulations. The Markov approach has a good validation score for downscaling (as is shown in Table 2), and the results can be further improved if the irradiance classification incorporates more than the clearness index, as well as the variability index [45], so as to better represent the variability of the distribution (especially the low variability periods). Moreover, the Markov approach introduces model complexity due to the higher-order dependencies in the data, which yield more accurate results but require greater computational effort. Several models that use the Markov approach considered the first-order Markov model for reducing the approach's complexity [40–45,52]. Even though the interrelated dependencies of the irradiance data can be better captured through a higher-order Markov model (a higher-order Markov model is described in Appendix C). Most authors who have used the Markov model also omit the seasonality and cloud effects on solar irradiance, which makes it non-stationary [129]. Applying a Markov model without properly handling the non-stationarity of the data can lead to inaccurate predictions and unreliable results. As a novel method, the non-dimensional approach employed by Peruchena et al. [79] and further developed by Larrañeta et al. [61] proved promising as a result of its simplicity, applicability, and versatility. Larrañeta et al. [61] compared to the stochastic adaptation of the method by Polo et al. [63] and the non-dimensional approach. The authors conclude that even though the non-dimensional approach offers a better performance in terms of the distribution of the synthetic data, it is less effective with respect to autocorrelation and the NRMSE compared to the stochastic adaptation. The Köppen–Geiger weather classification database of the non-dimensional approach made it globally applicable. Even though it has a lower number of occurrences in the literature than the stochastic approach, the non-dimensional one is a single method, whereas the stochastic approach is a combination of different methods using some special stochastic processes. The machine learning algorithm is emerging and still being developed, even though several other models

Fig. 9. **(a)** Trends in the literature on solar downscaling approaches comprising non-dimensional (ND), stochastic, and machine learning (ML) approaches; **(b)** trends in the sub-hourly resolution or high frequency wind speed time series literature from Scopus (https://www.scopus.com). The lines represent the number of publications per year and the dotted lines are the trends of the methods.

Table 1
Qualitative comparison of the solar downscaling approaches based on simplicity, comprehension, modular error, the use of real irradiance values in the synthetic data, and computational expenses.

	Simple	Comprehensive	Modular error	Real data	Computational expenses
Deterministic	Yes ☑	No ☒	No ☑	No ☒	Low ☑
Stochastic	No ☒	Yes ☑	Yes ☒	No ☒	High ☒
Markov	No ☒	Yes ☑	Yes ☒	No ☒	High ☒
Non-dimensional	Yes ☑	Yes ☑	No ☑	Yes ☑	Low ☑
Machine learning	No ☒	Yes ☑	Yes ☒	No ☒	High ☒

have used machine learning in classifying the clearness index. Larrañeta et al. [61] in the non-dimensional model used KNN-supervised learning to classify the database for matching with the data to be downscaled. Machine learning was also utilized by Frimane et al. [51] for clustering purposes; that is, machine learning may not always be distinctly separated from other approaches. Unsupervised learning in the direction of neural networks is promising, as it was applied by Schreck et al. [93] and Tang et al. [104] with a relatively good NRMSE compared to the other methods analyzed (as is shown in Table 2). In addition to the machine learning approach described, the use of data imputation approaches for missing data values may also prove promising [130,131]. To further understand the strengths and weaknesses of the methods, the qualitative measures of each of the methods is shown in Table 1. The non-dimensional approach outperforms other approaches in terms of simplicity, comprehension, modular error, usage of real irradiance values in the synthetic data and computational expenses.

Different methods are presented in Table 2. The data table lists the solar methods used in the literature, their temporal resolutions, site-dependence (this constitutes a yes if the ground data of the location to be downscaled is required for the method), and validation shows the different error measurements between the synthetic and measured data, as discussed in section 4, with their unique approaches and error measurements capturing solar variability. One key development in the future could be a better way of capturing the variability as seen in Ruiz-Arias and Gueymard [132], and Larrañeta et al. [61], where variability, distribution, energy, and dynamic threshold are used as part of the classification process. The non-dimensional model could also increase its database beyond the five major Köppen–Geiger weather classifications, accommodate more explanatory variables, and use a better classfication method in aggregating the database for improvements in the methodology of the approach for a better synthesis. Although increasing the database will lead to a more computational runtime in the approach, a good compromise should be obtained. The non-dimensional approach has been shown to provide a good result in the validation metrics relative to other approaches (as shown in Table 2).

The curves in Fig. 9(b) show the plot and trend of the sub-hourly resolution and high-frequency wind speed time series data from the Scopus literature database. This suggests that even though few methods deal with the wind speed downscaling process, especially at the sub-hourly level, the concept of sub-hourly data on wind speed is gaining importance. Although wind data shows small intra-hour variability, in contrast to solar data (see Fig. 2), it requires a more complex distribution for an appropriate representation. The diurnal data can be represented by a two-factor Weibull distribution. The wind speed cannot be perfectly modeled by pure statistics, which is why different methods have therefore modeled wind speed as the combination of meteorological reanalysis and stochastic simulations (see section 3.2). Even though the PSD has been shown to give good accuracy in modeling or downscaling wind time series, intense work is still needed to capture wind fluctuation, which is turbulent at an arbitrary height.

6. Conclusions

The methods for increasing the temporal resolution of solar and wind data presented in this paper demonstrate the growing effort to simulate finely resolved data in the field of energy system modeling to improve both the accuracy and reliability of the model results. Even though a plethora of methods have been developed in recent years, a systematic literature review was, up until now, lacking. We sought to close this research gap by systematically assessing the methods found in the literature and categorizing them into Markov, non-dimensional, deterministic, stochastic, and machine learning approaches for solar irradiance. Then, conventional methods for interpolations and statistics were employed, as well as simulations based on power spectral density in wind speed time series. These methods exhibit plausible results with respect to their capability of mimicking and predicting the statistical features of the real observable time series of renewable energy sources. Thus, they have the potential to accurately simulate or even reproduce the intra-hour variability of solar irradiance and wind speed data. Such data can be used in future research to also make energy system models at the sub-hourly scale reliable and therefore close the gap between modeling and real system dynamics. However, it is important to note that each of the methods has its strengths and limitations, and further research is needed to fully understand the best approach for increasing the temporal resolution of solar irradiance and wind speed time series data. All things considered, the non-dimensional approach for irradiance is uncomplicated with global applicability, and yet a robust methodology yielded good validation scores in root mean square error and Kolmogorov–Smirnov integral tests. Similarly, the method of combining the meteorological reanalysis and stochastic fluctuations for wind speed outperformed the conventional methods of interpolations and statistics.

In light of these findings, the following recommendations could be helpful for future researchers with respect to the existing methods:

I. As the downscaling of solar irradiance greatly depends on the clearness index of the irradiance, a better approach to classifying the clearness index and better capturing the variability could be employed in the models. In addition to the clearness, the variability index could also be further investigated.
II. Potential future research in the machine learning approach could explore options for capturing the variability through different indices for better reproducibility of the synthetic data. Moreover, the concept of data imputation using neural networks could be explored to fill in the assumed data gaps in the coarse time series data.
III. The non-dimensional approach could be improved by using other classification methods. Thus far, the non-dimensional models have used the K-nearest neighbour algorithm to classify the irradiance, as in the latest work by Larrañeta et al. [61].
IV. The power spectral density of the wind speed could also be further enhanced by improving the capturing of wind speed for different heights considering turbulence.

More highly resolved data bases and meteorological reanalyses in the future will be able to capture some coarse sub-hourly data, as seen in the National Solar Radiation Database, Table 3, which captures data up to 10 min intervals for some locations. This input could further improve the accuracy of future approaches as:

I. High-resolution data enhances the accuracy of the reviewed methods by capturing fine-scale variability.
II. Meteorological models continue to advance and achieve higher levels of maturity and resolution, and may reach a point at which they completely replace the reviewed methods. This is due to the holistic approach they follow, which considers the spatiotemporal scenarios, which are underpinned by a fundamental thermodynamic model.

Future research should be able to address the question of which accuracy indicators in the input data space (the solar and wind data) are relevant for energy system models, e.g., do we really need perfectly valid reanalyzed climate data, or is it more about the spotting of potentially extreme situations at the sub-hourly scale that are relevant for a robust system design? Therefore, the approaches can be tested in an energy system model for accuracy indications to observe the impact on the overall objective functions, parameters, and capacities.

Declaration of competing interest

The authors declare that they have no known competing financial interests or personal relationships that could have appeared to influence the work reported in this paper.

Data availability

The authors do not have permission to share data.

Acknowledgements

This work was supported by the Helmholtz Association under the program, "Energy System Design". We would like to acknowledge the Dipartimento di Energia, Politecnico di Milano for the measured solar irradiance data provision. We would also like to acknowledge and express our gratitude to M. Larrañeta, C. Fernandez-Peruchena, M. A. Silva-Pérez, and I. Lillo-Bravo for granting permission to reprint Figs. 5 and 6 from their work, 'Methodology to synthetically downscale DNI time series from 1-h to 1-min temporal resolution with geographic flexibility' Copyright (2018), with permission from Elsevier.

Appendix A

Table 2
Solar methods used in the literature, their temporal resolutions, site dependence (this constitutes a 'yes' if the ground data of the location to be downscaled is required for the method), and validation shows the different error measurements between the synthetic and measured data, as discussed in section 4 (the rows with a "c" in the validation show the confidence limits, e.g., 'KSI = 99%c').

Year	Authors	Renewable	Temporal resolution	Methods	Site dependence	Validation
2010	Beyer et al. [73]	DNI	1 h – 1 min	Stochastic model	No	–
2011	Polo et al. [63]	GHI & DNI	1 h – 10 min	Stochastic model	No	RMSE: <5%
2013	Grantham et al. [67]	DNI	1 h – 5 min	Stochastic model	No	NRMSE: 16.3% MBD: 0.4%
2013	Wey et al. [69]	GHI & DNI	1 h – 10 min	Stochastic model	Yes	RMSE: 18.6% KSI: <71%
2014	Hofmann et al. [40]	GHI	1 h – 1 min	Markov model	No	RMSE: <25%
2014	Ngoko et al. [39]	GHI	1 h – 1 min	Markov model	No	SD Mean
2014	Fernandez-Peruchena et al. [79]	DNI	1 h – 1 min	ND model	Yes	KSI: ~20%
2015	Fernandez-Peruchena et al. [53]	DNI	1 h – 1 min	ND model	Yes	NRMSE: <22% KSI: <23%
2015	Fernandez-Peruchena et al. [80]	DNI	1 h – 1 min	ND model	Yes	RMSE: <22% KSI: <22.9%
2015	Larra ñ eta et al. [62]	GHI & DNI	1 h – 10 min	Stochastic model	No	RMSE: 8%
2015	Bright et al. [41]	GHI	1 h – 1 min	Markov model	No	RMSE: 1.5% KSI: ~99%c
2015	Bright et al. [42]	GHI	1 h – 1 min	Stochastic model	No	KSI: ~99%c
2016	Fernandez-Peruchena et al. [81]	GHI	1 h – 1 min	ND model	Yes	RMSE: 11.6% KSI: <8%
2016	McDowell and Kummert [54]	GHI	1 h – 5 min	Deterministic model	No	RMSE: <11.4%
2016	Perry and Troccoli [72]	GHI	1 h – 1 min	Stochastic model	No	KSI: <3.9%
2016	Pereira et al. [60]	GHI	1 h – 30min	Deterministic model	No	-
2016	Poole and Dinter [84]	DNI	1 h – 1 min	ND model	Yes	KSI: ~3%
2017	Bright et al. [44]	GHI & DNI	1 h – 1 min	Markov model	No	RMSE: 1% KSI: 99%c
2017	Bright J.M. [43]	GHI & DNI	1 h – 1 min	Markov model	No	RMSE: 1% KSI: 99%c
2017	Grantham et al.[68]	GHI & DNI	1 h – 5 min	Stochastic model	No	NRMSE: ~2%
2017	Fernandez-Peruchena et al. [83]	DNI	3 h – 1 min	ND model	Yes	KSI: 6%
2018	Larra ñ eta M. [85]	DNI	1 h – 1 min	Stochastic and ND models	No	NRMSE: 3.4% NRMSE: 0.9%
2018	Fernandez- Peruchena et al. [82]	GHI & DNI	1 h – 1 min	ND model	Yes	KSI: ~70%
2018	McDowell et al. [55]	GHI & DNI	1 h – 1 min	Deterministic model	No	RMSE: <25%
2018	Inacio and Borges [52]	GHI & DNI	1 h – 1 min	Markov model	No	KSI: 1%
2018	Larra ñ eta et al. [61]	DNI	1 h – 1 min	Stochastic and ND models	No	NRMSE: 3.4% NRMSE: 0.9%
2018	Shi et al. [50]	GHI	1 h – 1 min	Markov model	No	KSI: ~95%c
2018	Zhang et al. [59]	GHI	30 min – 1 min	Stochastic model	No	MSE
2019	Zhang et al. [56]	GHI	30 min – 1 min	Stochastic model	No	–

(continued on next page)

Table 2 (*continued*)

Year	Authors	Renewable	Temporal resolution	Methods	Site dependence	Validation
2019	Bright J.M. [45]	GHI	1 h – 1 min	Markov model	No	RMSE: <7% KSI: 95%c
2019	Widén and Munkhammar [75]	GHI	1 h – 15 s	Stochastic model	No	–
2019	Frimane et al. [51]	GHI	10 min – 1 min	Markov model	No	NRMSE: <4%
2019	Larra ñ eta et al. [86]	GHI & DNI	1 h – 1 min	ND model	No	RMSE KSI: 5.8%
2020	Schreck et al. [93]	GHI & DNI	1 h – 1 min	Machine learning	No	–
2020	Keeratimahat et al. [71]	GHI & DNI	1 h – 4 s	Stochastic model	No	KSI: <80%
2020	Frimane et al. [70]	GHI	1 h – 1 min	Stochastic model	No	KLD OVC
2021	Tang et al. [104]	PV/load power	30 min or 1 hr – 5 min	Machine learning	No	NRMSE: 0.3%
2021	Martins et al. [47]	GHI	1 h – 1 min	Markov model	No	MSE: 1.5%
2021	Buster et al. [57]	GHI & DNI	30 min – 1 min & 5 min	Deterministic model	No	RMSE: <31.6%
2021	Zhang et al. [74]	GHI	30 min – 1 min	Stochastic model	No	Autocorrelation: 95%
2022	Larra ñ eta et al. [87]	GHI & DNI	1 h – 1 min	ND model	No	KSI
2022	Jim é nez-Valero et al. [89]	GHI & DNI	1 h – 1 min	ND model	No	KSI
2022	Huang et al. [76]	GHI	1 h – 1 min	Stochastic model	No	–
2022	Ruiz-Arias J.A. [64]	GHI	1 h – 1 min	Deterministic model	No	–
2022	Munkhammar and Widén [48,49]	GHI	1 h – 1 min	Markov model	Yes	KSI
2023	Kreuwel et al. [106]	GHI	1 h – 1 min	Machine learning	No	–
2023	Balog et al. [65]	GHI	1 h – 1 min	Deterministic model	No	MBD: 0.4% RMSE: 31.8%

Appendix B

Table 3
Different open access meteorological databases, their temporal resolutions, and regions.

Name	Database	License	Temporal resolution	Years	Renewables	Developers	Regions
Renewable ninja [133,134]	NASA MERRA-2 reanalysis CM-SAF's SARAH dataset	CC BY-NC 4.0	1 h	2000–2018	Solar and Wind	ETH Zurich and the Imperial College of London	Global
EMHIRES [135]	MERRA-1	European commission reuse	1 h	1986–2015	Solar and Wind	European union	EU-28
Open power system data [136]	ENTSO-E	Creative Commons Attribution 4.0 International	15 min	2015–2020	Solar and Wind	Neon Neue Energiëokonomik TU Berlin ETH Zürich DIW Berlin	Europe
ERA5 Reanalysis [137]	ERA5	Creative Commons Attribution 4.0	1 h	1950–2020	Solar and Wind	University of Reading NCAS	Europe
MERRA2 Derived [138]	MERRA-2	Creative Commons Attribution 4.0 International	1 h	1980–2018	Solar and Wind	University of Reading	Europe
C3S [139]	ECMWF ERA5	ECMWF Copernicus License 1.0	1 h	1979–2022	Solar and Wind	–	Europe
NREL NSRDB [58]	NREL's PSM NOAA's GOES NIC's IMS NASA's MODIS MERRA-2	Creative Commons Attribution 3.0 United States License	5 min to 1 h (region dependent)	1998–2021 (region dependent)	Solar and Wind	NREL	Global
PECD (2021 update) for ENTSO-E [140]	ERA5 and Global Wind Atlas version 2	CC BY 4.0	1 h	1982–2019	Solar and Wind	Technical University of Denmark, Department of Wind and Energy Systems	Europe + neighboring regions

Appendix C. Markov Chain

A Markov chain is a mathematical method that can be used to produce a probabilistic model for a stochastic process. The Markov property is exhibited if the probability distribution of the future states of a process is conditionally-independent of the past of the process, other than the present [141]. The Markov property is also known as the memoryless property of a stochastic process. In the equation below, a process X with $(X_{t+1}, t = 0, 1, 2, \ldots)$ will be in state j at time t if $X_{t+1} = j$. Mathematically:

$$P_{ij} = P(X_{t+1} = j | X_1 = x_1, X_2 = x_2, \ldots, X_t = x_0) \quad \text{Eq. C. 1}$$

$$P_{ij} = P(X_{t+1} = j | X_t = i) \quad \text{Eq. C. 2}$$

where P_{ij} is the transition probability of the process from i to j with the assumption of the immediate future state depending on the present one. In other words, the present event depends only on the immediate past event. Eq. (C. 3) represents the first-order Markov process. In a condition in which the present event depends on the immediate past event and the one before, it is referred to as the second order Markov process, and so on.

$$P_{ij} = P(X_t = j | X_{t-1} = i)$$ Eq. C. 3

Eq. (C. 4) shows the probability of a process at state k depending only on the event of t-1, at state i, and t-2 at state j. Depending on the probability of an event linking i, j, and k, a Markov transition matrix or transition probability matrix is constructed that is an n × n dimensional matrix with n representing the number of states. The Markov transition matrix linking the states of m (1, 2, …,n) can be represented according to Ref. [39]:

$$P_{ijk} = P(X_t = k | X_{t-1} = i, X_{t-2} = j)$$ Eq. C. 4

The matrix above is in the first-order Markov process. The higher order Markov process for reaching state i from j is obtained by Eq. (C. 5):

$$P_{ijk}(n) = A_{ij}^{n}$$ Eq. C. 5

This means that the higher order is obtained by taking the power of the Markov transition matrix in that order. It is possible to move from state i to j with an intermediate stop at k after r steps by using the Chapman–Kolmogorov theorem, which is possible through the exploitation of Markov's property.

The hidden Markov model is a type of machine learning algorithm that can be used to predict the future behavior of a sequence of events. It is a probabilistic model that can be used to model a variety of sequential events including text processing, speech recognition, and vision recognition. A hidden Markov model uses probabilistic distributions to model different states of a system at each step in a sequence. These states are known as hidden states, the probability of each determining whether the system is in a particular state at a given time. The system transitions from one state to another based on the state probabilities and the current state, whereas the probabilities are represented by the Markov transition matrix. To generate the prediction of a hidden Markov model, the identification of the probability distribution of the hidden states of the system over time is needed. For this, a hidden Markov model must be fitted to the data that represents the sequence of observations of the system over a period of time. If there are sets of hidden variables $X_1, X_2, \ldots, X_n$ and observed variables $Y_1, Y_2, \ldots, Y_n$, we can obtain the probability of X given Y:

$$P = P(X_1, X_2, \ldots, X_n | Y_1, Y_2, \ldots, Y_n)$$ Eq. C. 6

This can then be converted using Baye's theorem:

$$\mathrm{P} = \frac{P(Y|X)}{P(X)P(Y)}$$ Eq. C. 7

References

[1] Unfccc C. "Paris agreement," FCCCC/CP/2015/L. 9/Rev. 1 [Online]. Available: https://unfccc.int/resource/docs/2015/cop21/eng/l09r01.pdf; 2015.

[2] Liu Z, Deng Z, Davis S, Ciais P. Monitoring global carbon emissions in 2022. Nat Rev Earth Environ 2023;4(4):205–6. https://doi.org/10.1038/s43017-023-00406-z.

[3] Commission E. The European green deal. Eur Community 2019;53:24 [Online]. Available: https://eur-lex.europa.eu/legal-content/EN/TXT/?uri=CELEX:52019DC0640.

[4] Kuhla B, Viereck G. Enteric methane emission factors, total emissions and intensities from Germany's livestock in the late 19th century: a comparison with the today's emission rates and intensities. Sci Total Environ Elsevier 2022;848:157754. https://doi.org/10.1016/j.scitotenv.2022.157754.

[5] Vasilakos PN, et al. US clean energy futures—air quality benefits of zero carbon energy policies. Atmosphere 2022;13:1401. https://doi.org/10.3390/atmos13091401.

[6] Liu Z, et al. Challenges and opportunities for carbon neutrality in China. Nat Rev Earth Environ 2022;3:141–55. https://doi.org/10.1038/s43017-021-00244-x.

[7] "Affirming Australia's net zero emissions by 2050 target.". https://www.dcceew.gov.au/about/news/affirming-australias-net-zero-emissions-by-2050-target. March 23, 2023.

[8] Dharmala N, et al. Win-win transportation strategies for India: linking air pollution and climate mitigation. Energy and Clim Change 2022;3:100072. https://doi.org/10.1016/j.egycc.2022.100072.

[9] Nakata T. Energy-economic models and the environment. Prog Energy Combust Sci 2004;30:417–75. https://doi.org/10.1016/j.pecs.2004.03.001.

[10] Lu Y, Khan ZA, Alvarez-Alvarado MS, Zhang Y, Huang Z, Imran M. A critical review of sustainable energy policies for the promotion of renewable energy sources. Sustainability 2020;12:5078. https://doi.org/10.3390/su12125078.

[11] Hoffmann M, Kotzur L, Stolten D, Robinius M. A review on time series aggregation methods for energy system models. Energies 2020;13:641. https://doi.org/10.3390/en13030641.

[12] Fernández-Blanco Carramolino R, Careri F, Kavvadias K, Hidalgo-Gonzalez I, Zucker A, Peteves E. "Systematic mapping of power system models,". Joint Res Cent (Eur Comm), Publ Off Eur 2017. https://doi.org/10.2760/422399. *URL*, https://ec.europa.eu/jrc/en/publication/systematic-mapping-powersystem-models-expert-survey.

[13] Welder L, Ryberg DS, Kotzur L, Grube T, Robinius M, Stolten D. Spatio-temporal optimization of a future energy system for power-to-hydrogen applications in Germany. Energy 2018;158:1130–49. https://doi.org/10.1016/j.energy.2018.05.059.

[14] Gelaro R, et al. The modern-era retrospective analysis for research and applications, version 2 (MERRA-2). J Clim 2017;30:5419–54. https://doi.org/10.1175/JCLI-D-16-0758.1.

[15] Hirth L, Mühlenpfordt J, Bulkeley M. The ENTSO-E Transparency Platform – a review of Europe's most ambitious electricity data platform. Appl Energy 2018;225:1054–67. https://doi.org/10.1016/j.apenergy.2018.04.048.

[16] Pfenninger S. Dealing with multiple decades of hourly wind and PV time series in energy models: a comparison of methods to reduce time resolution and the planning implications of inter-annual variability. Appl Energy 2017;197:1–13. https://doi.org/10.1016/j.apenergy.2017.03.051.

[17] Weinand JM, Hoffmann M, Göpfert J, Terlouw T, Schönau J, Kuckertz P, et al. Global LCOEs of decentralized off-grid renewable energy systems. Renew Sustain Energy Rev 2023;183:113478. https://doi.org/10.1016/j.rser.2023.113478.

[18] Sonia Leva AN, Alfredo Nespoli, Silvia Pretto, Marco Mussetta, Emanuele Ogliari. Photovoltaic power and weather parameters. 2020. https://doi.org/10.21227/42v0-jz14.

[19] Gangammanavar H, Sen S, Zavala VM. Stochastic optimization of sub-hourly economic dispatch with wind energy. IEEE Trans Power Syst 2015;31:949–59. https://doi.org/10.1109/TPWRS.2015.2410301.

[20] Troy N, Flynn D, O'Malley M. The importance of sub-hourly modeling with a high penetration of wind generation. In: 2012 IEEE power and energy society general meeting; 2012. p. 1–6. https://doi.org/10.1109/PESGM.2012.6345631.

[21] O'Dwyer C, Flynn D. Using energy storage to manage high net load variability at sub-hourly time-scales. IEEE Trans Power Syst 2014;30:2139–48. https://doi.org/10.1109/TPWRS.2014.2356232.

[22] Lopez ID, Flynn D, Desmartin M, Saguan M, Hinchliffe T. "Drivers for sub-hourly scheduling in unit commitment models,". In: 2018 IEEE power & energy society general meeting (PESGM); 2018. p. 1–5. https://doi.org/10.1109/PESGM.2018.8586262.

[23] Meybodi MA, Santigosa LR, Beath AC. A study on the impact of time resolution in solar data on the performance modelling of CSP plants. Renew Energy 2017;109:551–63. https://doi.org/10.1016/j.renene.2017.03.024.

[24] Ernst M, Gooday J. Methodology for generating high time resolution typical meteorological year data for accurate photovoltaic energy yield modelling. Sol Energy 2019;189:299–306. https://doi.org/10.1016/j.solener.2019.07.069.

[25] Mayer MJ. Effects of the meteorological data resolution and aggregation on the optimal design of photovoltaic power plants. Energy Convers Manag 2021;241:114313. https://doi.org/10.1016/j.enconman.2021.114313.

[26] Hofmann M, Seckmeyer G. Influence of various irradiance models and their combination on simulation results of photovoltaic systems. Energies 2017;10:1495. https://doi.org/10.3390/en10101495.

[27] Salom J, Widén J, Candanedo J, Lindberg KB. Analysis of grid interaction indicators in net zero-energy buildings with sub-hourly collected data. Adv Build Energy Res 2015;9:89–106. https://doi.org/10.1080/17512549.2014.941006.

[28] Deane JP, Drayton G, Gallachóir BPÓ. The impact of sub-hourly modelling in power systems with significant levels of renewable generation. Appl Energy 2014;113:152–8. https://doi.org/10.1016/j.apenergy.2013.07.027.

[29] Bistline JET. The importance of temporal resolution in modeling deep decarbonization of the electric power sector. Environ Res Lett 2021;16:084005. https://doi.org/10.1088/1748-9326/ac10df.

[30] Kërçi T, Giraldo J, Milano F. Analysis of the impact of sub-hourly unit commitment on power system dynamics. Int J Electr Power Energy Syst 2020; 119:105819. https://doi.org/10.1016/j.ijepes.2020.105819.
[31] Kazemi M, Siano P, Sarno D, Goudarzi A. Evaluating the impact of sub-hourly unit commitment method on spinning reserve in presence of intermittent generators. Energy 2016;113:338–54. https://doi.org/10.1016/j.energy.2016.07.050.
[32] Zurita A, Mata-Torres C, Cardemil JM, Escobar RA. Assessment of time resolution impact on the modeling of a hybrid CSP-PV plant: a case of study in Chile. Sol Energy 2020;202:553–70. https://doi.org/10.1016/j.solener.2020.03.100.
[33] Hoffmann M, Kotzur L, Stolten D. The Pareto-optimal temporal aggregation of energy system models. Appl Energy 2022;315:119029. https://doi.org/10.1016/j.apenergy.2022.119029.
[34] Hoffmann M, Priesmann J, Nolting L, Praktiknjo A, Kotzur L, Stolten D. Typical periods or typical time steps? A multi-model analysis to determine the optimal temporal aggregation for energy system models. Appl Energy 2021;304:117825. https://doi.org/10.1016/j.apenergy.2021.117825.
[35] Page MJ, et al. The PRISMA 2020 statement: an updated guideline for reporting systematic reviews. Int J Surg 2021;88:105906. https://doi.org/10.1136/bmj.n71.
[36] Antonanzas-Torres F, Urraca R, Polo J, Perpiñán-Lamigueiro O, Escobar R. Clear sky solar irradiance models: a review of seventy models. Renew Sustain Energy Rev 2019;107:374–87. https://doi.org/10.1016/j.rser.2019.02.032.
[37] Correa LF, Folini D, Chtirkova B, Wild M. A method for clear-sky identification and long-term trends assessment using daily surface solar radiation records. Earth Space Sci 2022;9. https://doi.org/10.1029/2021EA002197. e2021EA002197.
[38] Stein JS, Hansen CW, Reno MJ. Global horizontal irradiance clear sky models: implementation and analysis (No. SAND2012-2389). Albuquerque, NM, and Livermore, CA (United States): Sandia National Laboratories (SNL); 2012. https://doi.org/10.2172/1039404.
[39] Ngoko BO, Sugihara H, Funaki T. Synthetic generation of high temporal resolution solar radiation data using Markov models. Sol Energy 2014;103: 160–70. https://doi.org/10.1016/j.solener.2014.02.026.
[40] Hofmann M, Riechelmann S, Crisosto C, Mubarak R, Seckmeyer G. Improved synthesis of global irradiance with one-minute resolution for PV system simulations. Int J Photoenergy 2014;2014. https://doi.org/10.1155/2014/808509.
[41] Bright JM, Smith CJ, Taylor PG, Crook R. Stochastic generation of synthetic minutely irradiance time series derived from mean hourly weather observation data. Sol Energy 2015;115:229–42. https://doi.org/10.1016/j.solener.2015.02.032.
[42] Bright J, Crook R, Taylor PG. Methodology to stochastically generate synthetic 1-minute irradiance time-series derived from mean hourly weather observational data. In: Proceedings of the ISES solar world congress 2015; 2016. p. 142–51. https://doi.org/10.18086/swc.2015.07.02.
[43] Bright JM. Development of a synthetic solar irradiance generator that produces time series with high temporal and spatial resolutions using readily available mean hourly observations," Ph.D. dissertation. 2017 [Online]. Available: https://etheses.whiterose.ac.uk/17610/.
[44] Bright JM, Babacan O, Kleissl J, Taylor PG, Crook R. A synthetic, spatially decorrelating solar irradiance generator and application to a LV grid model with high PV penetration. Sol Energy 2017;147:83–98. https://doi.org/10.1016/j.solener.2017.03.018.
[45] Bright JM. The impact of globally diverse GHI training data: evaluation through application of a simple Markov chain downscaling methodology. J Renew Sustain Energy 2019;11:023703. https://doi.org/10.1063/1.5085236.
[46] Munkhammar J, Widén J. An N-state Markov-chain mixture distribution model of the clear-sky index. Sol Energy 2018;173:487–95. https://doi.org/10.1016/j.solener.2018.07.056.
[47] Martins FR, Soares TG, Lima FJL. Generating solar irradiance data series with 1-minute time resolution based on hourly observational data. IEEE Latin Am Trans 2021;19(2):191–8. https://doi.org/10.1109/TLA.2021.9443060.
[48] Munkhammar J, Widén J. Modeling combined global, beam, and diffuse clear-sky indices with Markov-chain mixture distribution models. J Renew Sustain Energy 2021;13(6). https://doi.org/10.1063/5.0071585.
[49] Munkhammar J, Widén J. "Downscaling global, beam and diffuse horizontal irradiance based on hour resolution global horizontal irradiance using Markov mixture distribution modeling,". in 21st Wind & Solar Integration Workshop (WIW 2022) 2022;2022:662–7. https://doi.org/10.1049/icp.2022.2838.
[50] Shi X, Acord B, Wang P. Incorporating ground-measured pollution observations to improve temporally downscaled solar irradiance simulations. Sol Energy 2018; 171:293–301. https://doi.org/10.1016/j.solener.2018.06.076.
[51] Frimane A, Soubdhan T, Bright JM, Aggour M. Nonparametric Bayesian-based recognition of solar irradiance conditions: application to the generation of high temporal resolution synthetic solar irradiance data. Sol Energy 2019;182:462–79. https://doi.org/10.1016/j.solener.2019.02.052.
[52] Inacio CO, Borges CLT. Stochastic model for generation of high-resolution irradiance data and estimation of power output of photovoltaic plants. IEEE Trans Sustain Energy 2017;9:952–60. https://doi.org/10.1109/TSTE.2017.2767780.
[53] Fernández-Peruchena CM, Blanco M, Gastón Mn, Bernardos A. Increasing the temporal resolution of direct normal solar irradiance series in different climatic zones. Sol Energy 2015;115:255–63. https://doi.org/10.1016/j.solener.2015.02.017.
[54] McDowell TP, Kummert M. Estimating sub-hourly solar radiation and effective sky temperature from hourly weather data. Proc SimBuild 2016;6 [Online]. Available: https://publications.ibpsa.org/conference/paper/?id=simbuild2016_C056.
[55] McDowell TP, Letellier-Duchesne S, Kummert M. A new method for determining sub-hourly solar radiation from hourly data. 2018 [Online]. Available: https://publications.ibpsa.org/conference/paper/?id=simbuild2018_C071.
[56] Zhang W, Kleiber W, Florita AR, Hodge B-M, Mather B. Modeling and simulation of high-frequency solar irradiance. IEEE J Photovoltaics 2018;9:124–31. https://doi.org/10.1109/JPHOTOV.2018.2879756.
[57] Buster G, Rossol M, Maclaurin G, Xie Y, Sengupta M. A physical downscaling algorithm for the generation of high-resolution spatiotemporal solar irradiance data. Sol Energy 2021;216:508–17. https://doi.org/10.1016/j.solener.2021.01.036.
[58] Sengupta M, Xie Y, Lopez A, Habte A, Maclaurin G, Shelby J. The national solar radiation data base (NSRDB). Renew Sustain Energy Rev 2018;89:51–60. https://doi.org/10.1016/j.rser.2018.03.003.
[59] Zhang W, Kleiber W, Florita AR, Hodge B-M, Mather B. A stochastic downscaling approach for generating high-frequency solar irradiance scenarios. Sol Energy 2018;176:370–9. https://doi.org/10.1016/j.solener.2018.10.019.
[60] Pereira S, Canhoto P, Salgado R. Spatial and temporal downscaling of solar global radiation and mean air temperature from weather forecast data-an introductory numerical study and validation. 2016 [Online]. Available: http://hdl.handle.net/10174/19385.
[61] Larrañeta M, Fernandez-Peruchena C, Silva-Pérez MA, Lillo-Bravo I. Methodology to synthetically downscale DNI time series from 1-h to 1-min temporal resolution with geographic flexibility. Sol Energy 2018;162:573–84. https://doi.org/10.1016/j.solener.2018.01.064.
[62] Larrañeta M, Moreno-Tejera S, Silva-Pérez MA, Lillo-Bravo I. An improved model for the synthetic generation of high temporal resolution direct normal irradiation time series. Sol Energy 2015;122:517–28. https://doi.org/10.1016/j.solener.2015.09.030.
[63] Polo J, Zarzalejo LF, Marchante R, Navarro AA. A simple approach to the synthetic generation of solar irradiance time series with high temporal resolution. Sol Energy 2011;85:1164–70. https://doi.org/10.1016/j.solener.2011.03.011.
[64] Ruiz-Arias JA. Mean-preserving interpolation with splines for solar radiation modeling. Sol Energy 2022;248:121–7. https://doi.org/10.1016/j.solener.2022.10.038.
[65] Balog I, Caputo G, Iatauro D, Signoretti P, Spinelli F. Downscaling of hourly climate data for the assessment of building energy performance. Sustainability 2023;15:2762. https://doi.org/10.3390/su15032762.
[66] Skartveit A, Olseth JA. The probability density and autocorrelation of short-term global and beam irradiance. Sol Energy 1992;49:477–87. https://doi.org/10.1016/0038-092X(92)90155-4.
[67] Grantham A, Pudney PJ, Boland JW, Belusko M. Synthetically interpolated five-minute direct normal irradiance. Australia Modelling and Simulation Society of Australia and New Zealand; 2013.
[68] Grantham AP, Pudney PJ, Ward LA, Belusko M, Boland JW. Generating synthetic five-minute solar irradiance values from hourly observations. Sol Energy 2017; 147:209–21. https://doi.org/10.1016/j.solener.2017.03.026.
[69] Wey E, et al. A fusion method for creating sub-hourly DNI-based TMY from long-term satellite-based and short-term ground-based irradiation data. Proc. SolarPACES; 2012 [Online]. Available: https://hal-mines-paristech.archives-ouvertes.fr/hal-00779770.
[70] Frimane Â, Bright JM, Yang D, Ouhammou B, Aggour M. Dirichlet downscaling model for synthetic solar irradiance time series. J Renew Sustain Energy 2020;12: 063702. https://doi.org/10.1063/5.0028267.
[71] Keeratimahat K, Copper J, Bruce A, MacGill I. Generation of synthetic 4 s utility-scale PV output time series from hourly solar irradiance data. J Renew Sustain Energy 2021;13:026301. https://doi.org/10.1063/5.0033855.
[72] Perry M, Troccoli A. An approach for generating synthetic fine temporal resolution solar radiation time series from hourly gridded datasets. Meteorol Z 2017;26:265–76. https://doi.org/10.1127/metz/2016/0746.
[73] Beyer H-G, Fauter M, Schumann K, Schenk H, Meyer R. Synthesis of DNI time series with sub-hourly time resolution. Proc SolarPACES 2010;2010 [Online]. Available: https://elib.dlr.de/67664/.
[74] Zhang W, Kleiber W, Hodge B-M, Mather B. A nonstationary and non-Gaussian moving average model for solar irradiance. Environmetrics 2022;33:e2712. https://doi.org/10.1002/env.2712.
[75] Widén J, Munkhammar J. Spatio-temporal downscaling of hourly solar irradiance data using Gaussian copulas. In: 2019 IEEE 46th photovoltaic specialists conference (PVSC); 2019. p. 3172–8. https://doi.org/10.1109/PVSC40753.2019.8980922.
[76] Huang J, Perez M, Perez R, Yang D, Keelin P, Hoff T. Nonparametric temporal downscaling of GHI clear-sky indices using Gaussian copula. In: 2022 IEEE 49th photovoltaics specialists conference (PVSC); 2022. p. 654–7. https://doi.org/10.1109/PVSC48317.2022.9938482.
[77] Lave M, Weekley A. Comparison of high-frequency solar irradiance: ground measured vs. satellite-derived. In: 2016 IEEE 43rd photovoltaic specialists conference (PVSC); 2016. p. 1101–6. https://doi.org/10.1109/PVSC.2016.7749784.
[78] Hummon M, Ibanez E, Brinkman G, Lew D. *Sub-hour solar data for power system modeling from static spatial variability analysis* (No. NREL/CP-6A20-56204). Golden, CO (United States): National Renewable Energy Lab.(NREL); 2012. https://www.osti.gov/servlets/purl/1059579.
[79] Peruchena CMF, Blanco M, Bernardos A. Generation of series of high frequency DNI years consistent with annual and monthly long-term averages using measured DNI data. Energy Proc 2014;49:2321–9. https://doi.org/10.1016/j.egypro.2014.03.246.

[80] Fernández-Peruchena C, Blanco M, Bernardos A. Increasing the temporal resolution of direct normal solar irradiance series in a desert location. Energy Proc 2015;69:1981–8. https://doi.org/10.1016/j.egypro.2015.03.199.
[81] Fernández-Peruchena CM, Gastón Mn. A simple and efficient procedure for increasing the temporal resolution of global horizontal solar irradiance series. Renew Energy 2016;86:375–83. https://doi.org/10.1016/j.renene.2015.08.004.
[82] Peruchena CF, Larrañeta M, Blanco M, Bernardos A. High frequency generation of coupled GHI and DNI based on clustered dynamic paths. Sol Energy 2018;159:453–7. https://doi.org/10.1016/j.solener.2017.11.024.
[83] Fernández-Peruchena CM, Gastón M, Schroedter-Homscheidt M, Marco IMn, Casado-Rubio JL, García-Moya JA. Increasing the temporal resolution of direct normal solar irradiance forecasted series. AIP Conf Proc 2017;1850:140007. https://doi.org/10.1063/1.4984515.
[84] Poole, I.V.; Dinter, F. (2016). "Increasing the temporal resolution of direct normal irradiance data using the South African Universities Radiometric Network". SASEC 2016, 4th Southern African Solar Energy Conference, 31 Oct – 2 Nov 2016, Stellenbosch, South Africa. [Online]. Available: https://sterg.sun.ac.za/wp-content/uploads/2010/11/77.pdf.
[85] Caminero MJLG. Synthetic generation of high-temporal resolution direct normal irradiation time series. Ph.D. dissertation; 2018. https://api.semanticscholar.org/CorpusID:139782693.
[86] Larrañeta M, Fernandez-Peruchena C, Silva-Pérez MA, Lillo-Bravo I, Grantham A, Boland J. Generation of synthetic solar datasets for risk analysis. Sol Energy 2019;187:212–25. https://doi.org/10.1016/j.solener.2019.05.042.
[87] Larrañeta M, Cantón-Marín C, Silva-Pérez MA, Lillo-Bravo I. Use of the ND tool: an open tool for the synthetic generation of 1-min solar data from hourly means with geographic flexibility. AIP Conf Proc 2022;2445:150002. https://doi.org/10.1063/5.0085901.
[88] Synthetic high-temporal resolution irradiance time series generator. http://estacionmeteo.us.gter.es/nd_model/validar_datos. [Accessed 29 May 2023].
[89] Jiménez-Valero P, et al. Synthetic generation of plausible solar years for long-term forecasting of solar radiation. Theor Appl Climatol 2022;150:649–61. https://doi.org/10.1007/s00704-022-04163-9.
[90] Moreno-Tejera S, Silva-Pérez MA, Ramírez-Santigosa L, Lillo-Bravo I. Classification of days according to DNI profiles using clustering techniques. Sol Energy 2017;146:319–33. https://doi.org/10.1016/j.solener.2017.02.031.
[91] Zou J, Han Y, So S-S. Overview of artificial neural networks. Artif Neural Networks 2008:14–22. https://doi.org/10.1007/978-1-60327-101-1_2.
[92] Dastres R, Soori M. Artificial neural network systems. Int J Imag Robot 2021;21:13–25 [Online]. Available: https://hal.science/hal-03349542.
[93] Schreck S, Schroedter-Homscheidt M, Klein M, Cao K-K. Satellite image-based generation of high frequency solar radiation time series for the assessment of solar energy systems. Meteorol Z 2020. https://doi.org/10.1127/metz/2020/1008.
[94] Schroedter-Homscheidt M, Kosmale M, Jung S, Kleissl J. Classifying ground-measured 1 minute temporal variability within hourly intervals for direct normal irradiances. Meteorol Z 2018;27:161–79. https://doi.org/10.1127/metz/2018/0875.
[95] Rodríguez E, Cornejo-Ponce L, Cardemil JM, Starke AR, Droguett EL. Estimation of one-minute direct normal irradiance using a deep neural network for five climate zones. Renew Sustain Energy Rev 2023;183:113486. https://doi.org/10.1016/j.rser.2023.113486.
[96] Mostafa BM, El-Attar N, Abd-Elhafeez S, Awad W. Machine and deep learning approaches in genome: review article. Alfarama J Basic & Appl Sci 2021;2(1):105–13. https://doi.org/10.21608/ajbas.2020.34160.1023.
[97] Goodfellow I, et al. Generative adversarial networks. Commun ACM 2020;63:139–44. https://doi.org/10.1145/3422622.
[98] Lu Y, Chen D, Olaniyi E, Huang Y. Generative adversarial networks (GANs) for image augmentation in agriculture: a systematic review. Comput Electron Agric 2022;200:107208. https://doi.org/10.1016/j.compag.2022.107208.
[99] Alqahtani H, Kavakli-Thorne M, Kumar G. Applications of generative adversarial networks (gans): an updated review. Arch Comput Methods Eng 2021;28:525–52. https://doi.org/10.1007/s11831-019-09388-y.
[100] Brophy E, Wang Z, She Q, Ward T. Generative adversarial networks in time series: a survey and taxonomy. *arXiv preprint arXiv:2107.11098*, https://doi.org/10.48550/arXiv.2107.11098; 2021.
[101] Chen Y, Li P, Zhang B. Bayesian renewables scenario generation via deep generative networks. In: 2018 52nd annual conference on information sciences and systems (CISS); 2018. p. 1–6. https://doi.org/10.1109/CISS.2018.8362314.
[102] Chen Y, Wang Y, Kirschen D, Zhang B. Model-free renewable scenario generation using generative adversarial networks. IEEE Trans Power Syst 2018;33:3265–75. https://doi.org/10.1109/TPWRS.2018.2794541.
[103] Fan H, Zhang X, Mei S. "Wind power time series missing data imputation based on generative adversarial network,". In: 2021 IEEE 4th international electrical and energy conference (CIEEC); 2021. p. 1–6. https://doi.org/10.1109/CIEEC50170.2021.9510923.
[104] Tang R, Dore J, Ma J, Leong PHW. Interpolating high granularity solar generation and load consumption data using super resolution generative adversarial network. Appl Energy 2021;299:117297. https://doi.org/10.1016/j.apenergy.2021.117297.
[105] Benti NE, Chaka MD, Semie AG. Forecasting renewable energy generation with machine learning and deep learning: current advances and future prospects. Sustainability 2023;15(9):7087. https://doi.org/10.3390/su15097087.
[106] Kreuwel FP, Knap W, Schmeits M, de Arellano JV-G, van Heerwaarden CC. Forecasting day-ahead 1-minute irradiance variability from numerical weather predictions. Sol Energy 2023;258:57–71. https://doi.org/10.1016/j.solener.2023.04.050.
[107] Karasu S, Altan A. Recognition model for solar radiation time series based on random forest with feature selection approach. In: 2019 11th international conference on electrical and electronics engineering (ELECO). IEEE; 2019. p. 8–11. https://doi.org/10.23919/ELECO47770.2019.8990664.
[108] Assaf AM, Haron H, Abdull Hamed HN, Ghaleb FA, Qasem SN, Albarrak AM. A review on neural network based models for short term solar irradiance forecasting. Appl Sci 2023;13(14):8332. https://doi.org/10.3390/app13148332.
[109] Horvath K, Bajić A, Ivatek-Šahdan S. Dynamical downscaling of wind speed in complex terrain prone to bora-type flows. J Appl Meteorol Climatol 2011;50(8):1676–91. https://doi.org/10.1175/2011JAMC2638.1.
[110] Kirchmeier MC, Lorenz DJ, Vimont DJ. Statistical downscaling of daily wind speed variations. J Appl Meteorol Climatol 2014;53(3):660–75. https://doi.org/10.1175/JAMC-D-13-0230.1.
[111] Shin J-Y, Jeong C, Heo J-H. A novel statistical method to temporally downscale wind speed Weibull distribution using scaling property. Energies 2018;11:633. https://doi.org/10.3390/en11030633.
[112] Carta JA, Ramírez P, Velázquez S. A review of wind speed probability distributions used in wind energy analysis: case studies in the Canary Islands. Renew Sustain Energy Rev 2009;13:933–55. https://doi.org/10.1016/j.rser.2008.05.005.
[113] Jung C, Schindler D. Wind speed distribution selection – a review of recent development and progress. Renew Sustain Energy Rev 2019;114:109290. https://doi.org/10.1016/j.rser.2019.109290.
[114] Carapellucci R, Giordano L. A methodology for the synthetic generation of hourly wind speed time series based on some known aggregate input data. Appl Energy 2013;101:541–50. https://doi.org/10.1016/j.apenergy.2012.06.044.
[115] Olauson J, Bergkvist M, Rydén J. Simulating intra-hourly wind power fluctuations on a power system level. Wind Energy 2016;20:973–85. https://doi.org/10.1002/we.2074.
[116] Correlations in renewable energy sources. https://corres.windenergy.dtu.dk. [Accessed 29 May 2023].
[117] Koivisto M, Jónsdóttir GM, Sørensen P, Plakas K, Cutululis N. Combination of meteorological reanalysis data and stochastic simulation for modelling wind generation variability. Renew Energy 2020;159:991–9. https://doi.org/10.1016/j.renene.2020.06.033.
[118] Murcia Leon JP, Koivisto MJ, Sørensen P, Magnant P. Power fluctuations in high-installation-density offshore wind fleets. Wind Energy Sci 2021;6:461–76. https://doi.org/10.5194/wes-6-461-2021.
[119] Schillebeeckx D, Leroy G. Generating long-term sub-hourly wind speed time series by coupling mesoscale models with full-scale spectra. J Phys Conf January 2022;2151:012003. https://doi.org/10.1088/1742-6596/2151/1/012003.
[120] Sørensen P, Hansen AD, Rosas PAC. Wind models for simulation of power fluctuations from wind farms. J Wind Eng Ind Aerod 2002;90(12–15):1381–402. https://doi.org/10.1016/S0167-6105(02)00260-X.
[121] Kumar J, Brooks B-GJ, Thornton PE, Dietze MC. Sub-daily statistical downscaling of meteorological variables using neural networks. Procedia Comput Sci 2012;9:887–96. https://doi.org/10.1016/j.procs.2012.04.095.
[122] Altan A, Karasu S, Zio E. A new hybrid model for wind speed forecasting combining long short-term memory neural network, decomposition methods and grey wolf optimizer. Appl Soft Comput 2021;100:106996. https://doi.org/10.1016/j.asoc.2020.106996.
[123] Valdivia-Bautista SM, Domínguez-Navarro JA, Pérez-Cisneros M, Vega-Gómez CJ, Castillo-Téllez B. Artificial intelligence in wind speed forecasting: a review. Energies 2023;16(5):2457. https://doi.org/10.3390/en16052457.
[124] Wang Y, Zou R, Liu F, Zhang L, Liu Q. A review of wind speed and wind power forecasting with deep neural networks. Appl Energy 2021;304:117766. https://doi.org/10.1016/j.apenergy.2021.117766.
[125] Karunasingha DSK. Root mean square error or mean absolute error? Use their ratio as well. Inf Sci 2022;585:609–29. https://doi.org/10.1016/j.ins.2021.11.036.
[126] Singla P, Duhan M, Saroha S. Different normalization techniques as data preprocessing for one step ahead forecasting of solar global horizontal irradiance. In: Artificial intelligence for renewable energy systems. Elsevier; 2022. p. 209–30. https://doi.org/10.1016/B978-0-323-90396-7.00004-3.
[127] Shi F, Hao Z, Shao Q. The analysis of water vapor budget and its future change in the Yellow-Huai-Hai region of China. J Geophys Res Atmos 2014;119(18). 10702-10719.
[128] Frimane Â, Bright JM. Synthetic solar irradiance: modeling solar data. "Validation of synthetic solar irradiance data,". Melville, New York: AIP Publishing; 2021. https://doi.org/10.1063/9780735421820_004. 4–1.
[129] Kumari P, Toshniwal D. Deep learning models for solar irradiance forecasting: a comprehensive review. J Clean Prod 2021;318:128566. https://doi.org/10.1016/j.jclepro.2021.128566.
[130] Lin W-C, Tsai C-F. Missing value imputation: a review and analysis of the literature (2006–2017). Artif Intell Rev 2020;53:1487–509. https://doi.org/10.1007/s10462-019-09709-4.
[131] Bülte C, Kleinebrahm M, Yilmaz HÜ, Gómez-Romero J. Multivariate time series imputation for energy data using neural networks. Energy and AI 2023;13:100239. https://doi.org/10.1016/j.egyai.2023.100239.
[132] Ruiz-Arias JA, Gueymard CA. CAELUS: classification of sky conditions from 1-min time series of global solar irradiance using variability indices and dynamic thresholds. Sol Energy 2023;263:111895. https://doi.org/10.1016/j.solener.2023.111895.

[133] Pfenninger S, Staffell I. Long-term patterns of European PV output using 30 years of validated hourly reanalysis and satellite data. Energy 2016;114:1251–65. https://doi.org/10.1016/j.energy.2016.08.060.
[134] Staffell I, Pfenninger S. Using bias-corrected reanalysis to simulate current and future wind power output. Energy 2016;114:1224–39. https://doi.org/10.1016/j.energy.2016.08.068.
[135] Gonzalez-Aparicio I, Zucker A, Careri F, Monforti F, Huld T, Badger J. EMHIRES dataset: wind and solar power generation. In: EMHIRES dataset: wind and solar power generation. Zenodo; 2021. https://doi.org/10.2760/044693.
[136] "open power system data.". https://data.open-power-system-data.org/time_series/2020-10-06. March 23, 2023.
[137] Bloomfield H, Brayshaw D. ERA5 derived time series of European aggregated surface weather variables, wind power, and solar power capacity factors: hourly data from 1950-2020. 2021. https://doi.org/10.17864/1947.000321.
[138] Bloomfield H, Brayshaw D, Charlton-Perez A. MERRA2 derived time series of European country-aggregate electricity demand, wind power generation and solar power generation. 2020. https://doi.org/10.17864/1947.239.
[139] Troccoli A, et al. The copernicus climate change service 'European climatic energy mixes. EMS Annu Meet 2017;14. EMS2017–824. [Online]. Available: https://hal-mines-paristech.archives-ouvertes.fr/hal-01583161.
[140] Koivisto MJ, Murcia Leon JP. Pan-European wind and solar generation time series (PECD 2021 update). In: Pan-European wind and solar generation time series (PECD 2021 update). Technical University of Denmark; 2022. https://doi.org/10.11583/DTU.c.5939581.v3.
[141] Gudivada VN, Rao D, Raghavan VV. Big data driven natural language processing research and applications. Handb Stat 2015;33:203–38. https://doi.org/10.1016/B978-0-444-63492-4.00009-5. Elsevier.